



**US Army Corps
of Engineers**
Waterways Experiment
Station

Technical Report IRRP-98-7
July 1998

Installation Restoration Research Program

Application of a Semianalytical Model to TNT Transport in Laboratory Soil Columns

by Tommy E. Myers, WES

*Dan M. Townsend, Benjamin C. Hill,
Louisiana State University*

WES

Approved For Public Release; Distribution Is Unlimited

Prepared for Headquarters, U.S. Army Corps of Engineers

The contents of this report are not to be used for advertising, publication, or promotional purposes. Citation of trade names does not constitute an official endorsement or approval of the use of such commercial products.

The findings of this report are not to be construed as an official Department of the Army position, unless so designated by other authorized documents.



PRINTED ON RECYCLED PAPER

Application of a Semianalytical Model to TNT Transport in Laboratory Soil Columns

by Tommy E. Myers

U.S. Army Corps of Engineers
Waterways Experiment Station
3909 Halls Ferry Road
Vicksburg, MS 39180-6199

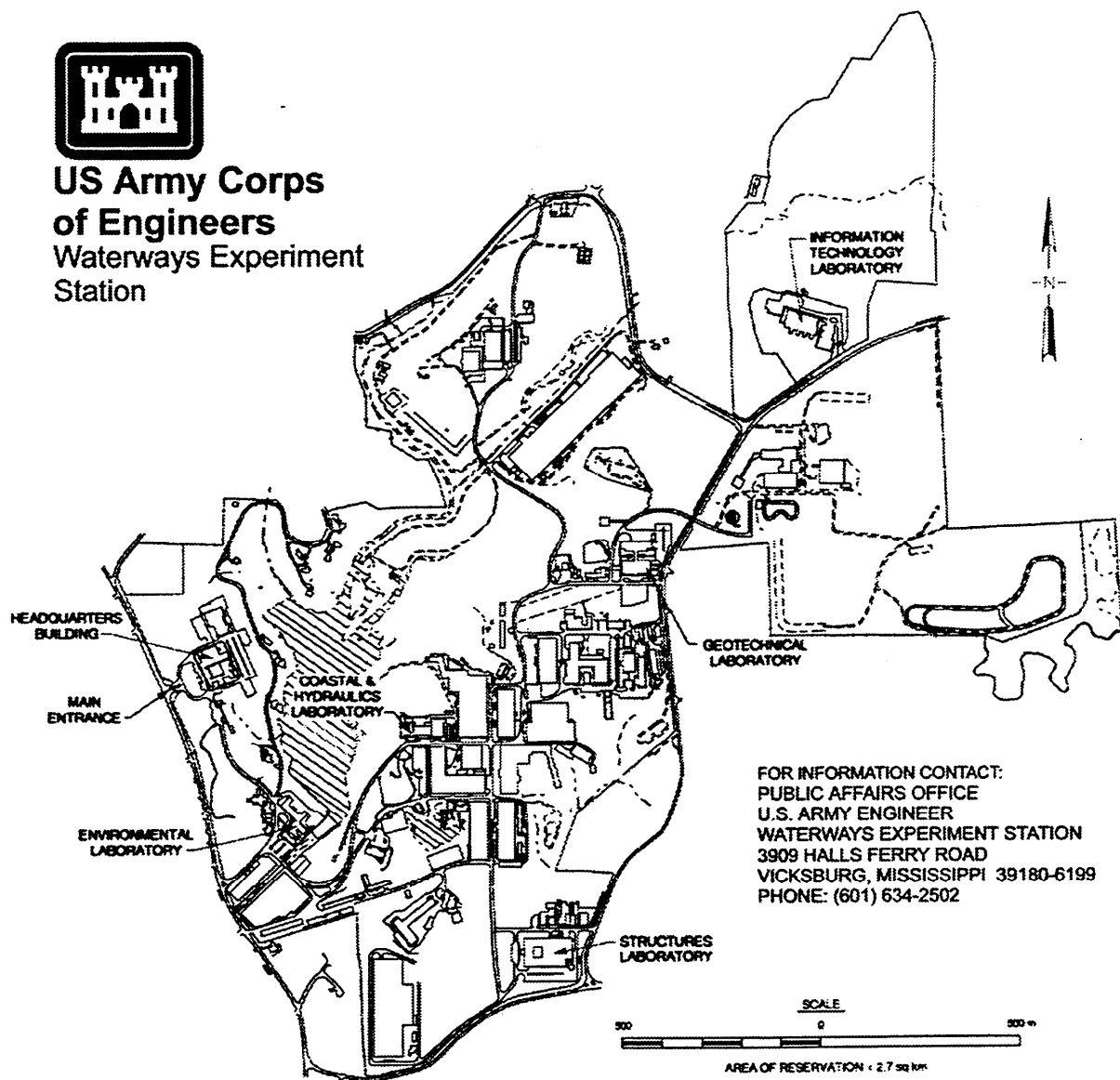
Dan M. Townsend, Benjamin C. Hill
Louisiana State University
Baton Rouge, LA 70803

Final report

Approved for public release; distribution is unlimited



**US Army Corps
of Engineers**
Waterways Experiment
Station



Waterways Experiment Station Cataloging-in-Publication Data

Myers, Tommy E.

Application of a semianalytical model to TNT transport in laboratory soil columns / by Tommy E. Myers, Dan M. Townsend, Benjamin C. Hill ; prepared for U.S. Army Corps of Engineers.

60 p. : ill. ; 28 cm. -- (Technical report ; IRRP-98-7)

Includes bibliographic references.

1. Partition coefficient (Chemistry) -- Mathematical models. 2. Soil absorption and adsorption -- Mathematical models. 3. Groundwater -- Pollution -- Mathematical models. 4. Soil pollution -- Mathematical models. I. Townsend, Dan M. II. Hill, Benjamin C. III. United States. Army. Corps of Engineers. IV. U.S. Army Engineer Waterways Experiment Station. V. Installation Restoration Research Program. VI. Series: Technical report (U.S. Army Engineer Waterways Experiment Station) ; IRRP-98-7. TA7 W34 no.IRRP-98-7

Contents

Preface	vi
1—Introduction	1
Background	1
Research Need	1
Purpose and Scope	4
2—Materials and Methods	5
Soil Column Breakthrough Curves	5
Semianalytical Model	14
3—Results and Discussion	20
Results	20
Discussion	37
4—Conclusions	39
References	40
Appendix A: Example of MathCad Implementations for Semianalytical Model	A1
SF 298	

List of Figures

Figure 1. Reduction pathways for 2,4,6-trinitrotoluene	2
Figure 2. Soil column test apparatus and soil column schematic	6
Figure 3. Soil A particle size distribution	7
Figure 4. Soil B particle size distribution	8
Figure 5. Soil C particle size distribution	9
Figure 6. Soil D particle size distribution	10
Figure 7. Observed and fitted chloride elution curves	14

Figure 8.	Comparison of the semianalytical solution to the analytical solution of Cleary and Adrian (1973)	21
Figure 9.	Comparison of the semianalytical solution to an analytical solution from Bear (1972)	21
Figure 10.	Comparison of the semianalytical solution to the numerical model of Grove and Stollenwerk (1984) for Freundlich sorption	22
Figure 11.	Comparison of the semianalytical solution to the numerical model of Grove and Stollenwerk (1984) for Langmuir sorption . .	22
Figure 12.	Observed and fitted TNT breakthrough curves for Soil A for linear sorption and first-order transformation	25
Figure 13.	Observed and fitted TNT breakthrough curves for Soil A for Freundlich sorption and first-order transformation	25
Figure 14.	Observed and fitted TNT breakthrough curves for Soil A for Langmuir sorption and first-order transformation	26
Figure 15.	Observed and fitted TNT breakthrough curves for Soil B for linear sorption and first-order transformation	27
Figure 16.	Observed and fitted TNT breakthrough curves for Soil B for Freundlich sorption and first-order transformation	27
Figure 17.	Observed and fitted TNT breakthrough curves for Soil B for Langmuir sorption and first-order transformation	28
Figure 18.	Observed and fitted TNT breakthrough curves for Soil C for linear sorption and first-order transformation	29
Figure 19.	Observed and fitted TNT breakthrough curves for Soil C for Freundlich sorption and first-order transformation	29
Figure 20.	Observed and fitted TNT breakthrough curves for Soil C for Langmuir sorption and first-order transformation	30
Figure 21.	Observed and fitted TNT breakthrough curves for Soil D for linear sorption and first-order transformation	31
Figure 22.	Observed and fitted TNT breakthrough curves for Soil D for Freundlich sorption and first-order transformation	32
Figure 23.	Observed and fitted TNT breakthrough curves for Soil D for Langmuir sorption and first-order transformation	32
Figure 24.	Observed and fitted TNT elution curves for Crane soil for linear sorption and first-order transformation	33
Figure 25.	Observed and fitted TNT elution curves for Crane soil for Freundlich sorption and first-order transformation	34
Figure 26.	Observed and fitted TNT elution curves for Crane soil for Langmuir sorption and first-order transformation	34

Figure 27.	Observed and fitted TNT elution curves for Crane soil for film diffusion, linear sorption, and first-order transformation	35
------------	--	----

List of Tables

Table 1.	Physical and Engineering Properties of Soils	5
Table 2.	Column Operating Parameters	11
Table 3.	Step Input Contaminant Concentrations	11
Table 4.	TNT Sorption and Transformation Parameters and <i>RMS</i> Values Estimated from the BTCs for Soils A, B, C, and D and from the Elution Curve for Crane Soil	36
Table 5.	TNT Mass Balance	36

Preface

The work reported herein was conducted by the U.S. Army Engineer Waterways Experiment Station (WES) for Headquarters, U.S. Army Corps of Engineers (HQUSACE). Funding was provided by the HQUSACE Installation Restoration Research Program (IRRP), Work Unit AF25-GW-002. Dr. Clem Myer was the IRRP Coordinator at the Directorate of Research and Development, HQUSACE. The HQUSACE Technical Monitors for Work Unit AF25-GW-003 were Messrs. David Becker and George O'Rourke. The IRRP Program Manager was Dr. M. John Cullinane.

This report was prepared by Mr. Tommy E. Myers, Environmental Restoration Branch (ERB), Environmental Engineering Division (EED), Environmental Laboratory (EL), WES; Mr. Dan M. Townsend, Contract-Graduate Student, (ERB); and Mr. Benjamin C. Hill, Contract Student, ERB. Chemical analyses were performed by the Environmental Chemistry Branch (ECB), EED. Physical analyses of the soils were performed by the Geotechnical Laboratory Soils Testing Facility, WES. Dr. D. Dean Adrian, Louisiana State University, Baton Rouge, LA, and Mr. Christian J. McGrath, Water Quality and Contaminant Modeling Branch, Environmental Processes and Effects Division (EPED), EL, were technical reviewers for this report.

The work was conducted under the direct supervision of Mr. Daniel E. Averett, Chief, ERB, and under the general supervision of Mr. Norman R. Francingues, Jr., Chief, EED, and Dr. John Harrison, Director, EL.

At the time of publication of this report, Dr. Robert W. Whalin was Technical Director of WES. Commander was COL Robin R. Cababa, EN.

This report should be cited as follows:

Myers, T. E., Townsend, D. M., and Hill, B. C. (1998). "Application of a semianalytical model to TNT transport in laboratory soil columns," Technical Report IRRP-98-7, U.S. Army Engineer Waterways Experiment Station, Vicksburg, MS.

The contents of this report are not to be used for advertising, publication, or promotional purposes. Citation of trade names does not constitute an official endorsement or approval of the use of such commercial products.

1 Introduction

Background

The Department of Defense is tasked with the cleanup of soils and groundwater at military installations. Many of these installations were involved in the manufacture and packing of 2,4,6-trinitrotoluene (TNT). As a result of these operations, subsurface contamination by TNT poses a potential threat to groundwater resources at many of these munitions facilities (Spaulding and Fulton 1988; Pugh 1982). To support remediation and containment efforts, technical guidance in modeling subsurface transport of TNT is needed.

Technical guidance for modeling the subsurface transport of TNT includes identification of applicable processes and the conditions for which these processes dominate. Many processes potentially affect subsurface transport of TNT, but the relative significance of individual processes varies. Technical guidance for modeling the subsurface transport of TNT also includes development of descriptors for significant processes and estimation of parameters used to quantify these descriptors. Valid process descriptors, along with good estimates of parameters used to quantify these descriptors, are vital to evaluation of various remediation and containment strategies.

Research Need

Sorption is a key process controlling TNT subsurface transport (Townsend and Myers 1996). Reductive transformations (Figure 1) are the most important degradation reactions affecting TNT subsurface transport (Townsend and Myers 1996). Recent research has led to a better understanding of the effects of these processes on TNT subsurface transport; however, many questions remain unanswered.

Column studies are laboratory-based physical models of contaminant transport in the subsurface and are often used to study contaminant transport processes. Column studies produce contaminant breakthrough curves (BTCs) when clean soils are challenged with contaminated water and/or contaminant elution curves when contaminated soils are challenged with clean water. In either case,

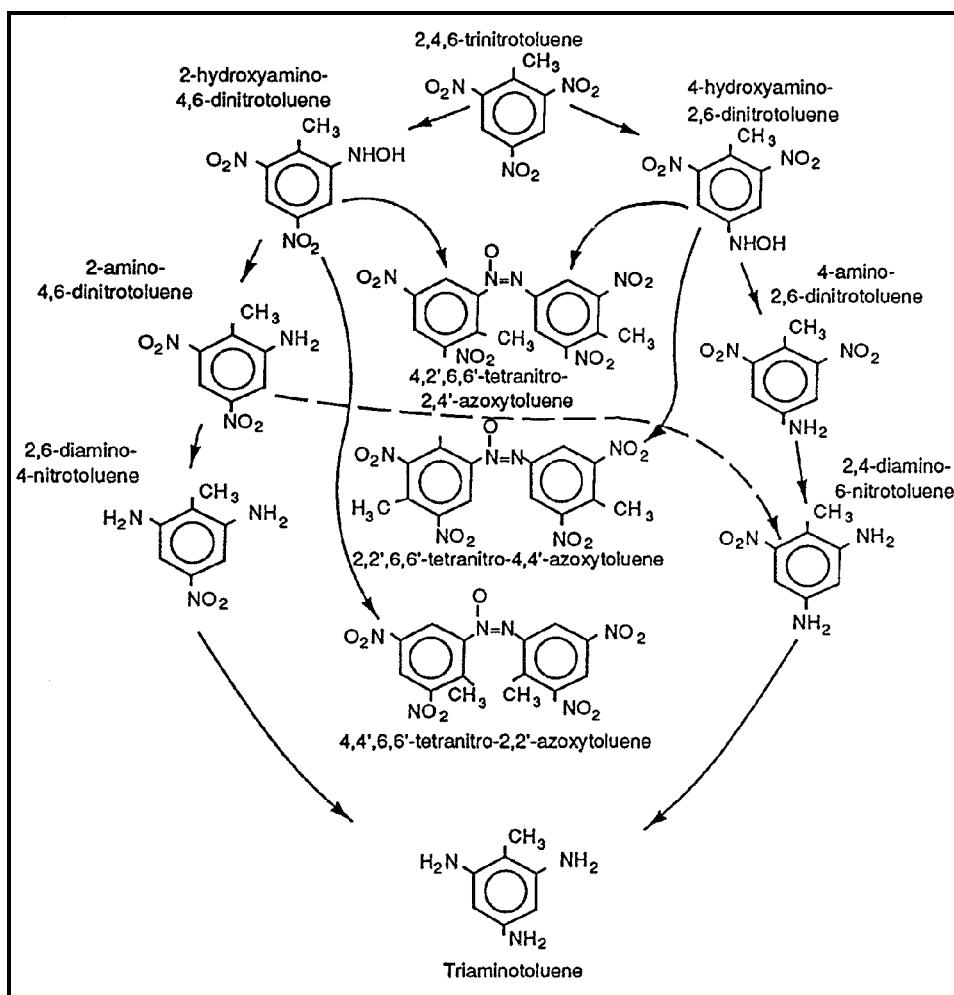


Figure 1. Reduction pathways for 2, 4, 6-trinitrotoluene (modified from McGrath 1995)

laboratory soil column data may be described by mathematical models in order to assess the contribution of each process modeled and to obtain fitted parameters. Satisfactory fitting of the model to the observations supports but does not prove the contention that all relevant processes have been described modeled adequately. However, failure to reproduce observations indicates omission of one or more significant processes from the model. Mathematical models used to simulate column data are usually based on the classical advection-dispersion equation and employ an analytical or numerical computation method. Column studies have been employed to investigate subsurface transport of TNT (Ainsworth et al. 1993; Comfort et al. 1995; Selim, Xue, and Iskandar 1995; Pennington et al. 1995; Townsend, Myers, and Adrian 1995; Olin, Myers, and Townsend 1996; Myers et al., In Preparation). Results of these studies have varied and so have modeling approaches.

Ainsworth et al. (1993) employed an analytical model with a linear equilibrium descriptor for sorption to simulate TNT BTCs. This model was unable to

capture the BTC asymmetry and mass loss shown by some of the BTCs. Ainsworth et al. (1993) also used models that accounted for (a) a slow first-order reversible reaction and linear sorption, (b) a slow first-order reversible reaction and nonlinear sorption, and (c) a first-order irreversible reaction. They found that none of the models were able to fully capture the asymmetry and mass loss observed in the BTCs.

Comfort et al. (1995) used an analytical model with a linear equilibrium descriptor coupled with a first-order transformation descriptor to simulate TNT BTCs. This model did not simulate the BTCs well due to BTC asymmetry. Since analytical solutions are limited to linear descriptors for sorption, Comfort et al. (1995) also used a numerical model (van Genuchten 1981) that included a nonlinear sorption descriptor (Freundlich isotherm) and first-order transformation. The numerical model with nonlinear sorption simulated the BTCs much better than the analytical solution with linear sorption.

Selim, Xue, and Iskandar (1995) also used a numerical model (Selim, Amacher, and Iskandar 1990) to simulate TNT BTCs. The numerical solution employed by these researchers, like the numerical solution used by Comfort et al. (1995), incorporated Freundlich sorption and first-order transformation and fit the data well.

Townsend, Myers, and Adrian (1995) and Olin, Myers, and Townsend (1996) used a complete-mix analytical model with linear equilibrium sorption and first-order transformation to simulate TNT BTCs obtained from short-length columns. The complete-mix analytical model simulated the BTCs well.

Myers et al. (In Preparation) used an analytical solution (van Genuchten and Alves 1982) that incorporated linear equilibrium sorption and first-order transformation to simulate TNT BTCs for sand, silt, and clay soils. The analytical solution simulated the sand BTC well, but failed to simulate the silt and clay BTCs.

Mathematical models are required for evaluating contaminant transport in laboratory soil column studies. Analytical models are of limited utility in many soil column studies because they are highly restrictive of the process descriptors that can be investigated. Analytical models, for example, are not available for nonlinear sorption and reaction terms. Numerical models are not limited to linear process descriptors, but numerical models are generally more difficult to implement than analytical models. Further, researchers that use numerical models tend to use their own codes, which may not be widely available, verifiable, or easy to modify. Since the literature indicates mixed success for analytical models, a model that is straightforward to implement, yet complex enough to accept nonlinear process descriptors, is needed for evaluating TNT laboratory soil column data.

Purpose and Scope

The purpose of this study was to evaluate the applicability of a one-dimensional, semianalytical solute transport model developed by Moldrup et al. (1992) and Yamaguchi et al. (1994) to TNT laboratory soil column studies. The Moldrup et al. (1992) and Yamaguchi et al. (1994) model incorporates linear and/or nonlinear reaction terms into the advection-dispersion equation. The semianalytical model was applied to TNT BTCs for four soils and to a TNT elution curve for a contaminated soil from a military installation. Application of the model to field problems was not investigated, nor was application of the model to contaminants other than TNT investigated.

2 Materials and Methods

Soil Column Breakthrough Curves

Soil column experiments were conducted in stainless steel columns (Figure 2), 15.24-cm length and 4.45-cm inside diameter. Four uncontaminated soils (A, B, C, and D) from the Louisiana Army Ammunition Plant (LAAP), Bossier City, LA, were used in the column studies. The four soils were excavated from various depths at the LAAP. Soil A was located between 2.4 and 3.4 m below the soil surface. Soil B was located between 3.7 and 4.6 m below the soil surface. Soil C was located between 1.2 and 2.3 m below the soil surface. Soil D was located between 2.3 and 3.5 m below the soil surface. Soils A, B, and C were silty sands, and Soil D was a sandy clay. Each soil was air-dried and passed through a 10-mesh screen. Physical and engineering properties of the soils are shown in Table 1, and grain-size distributions are shown in Figures 3, 4, 5, and 6 for Soils A, B, C, and D, respectively. Specific gravities, water contents, and hydraulic conductivities were determined according to methods described in U.S. Army Corps of Engineers (1970). Soils were loaded into the columns in two approximately equal lifts. The soil surface was scarified between lifts to minimize bedding planes. Flows (upflow mode) were set to provide average pore water velocities of about 10^{-4} cm/sec using constant-volume metering pumps (Model QG6-0-SSY, Fluid Metering, Inc., Oyster Bay, NY). Column operating parameters are provided in Table 2. Bulk densities were calculated from water content, total soil weight loaded, specific gravity, and column inside dimensions. Effective porosities were determined from chloride tracer studies as discussed later in the section on dispersion coefficients. Average pore water velocities were determined from effective porosities and column operating records.

Table 1
Physical and Engineering Properties of Soils

Soil	A	B	C	D
Specific Gravity	2.66	2.68	2.70	2.74
Water Content	0.008	0.008	0.021	0.043
Hydraulic Conductivity, cm/sec	3.17×10^{-4}	2.97×10^{-4}	7.75×10^{-7}	$< 10^{-9}$

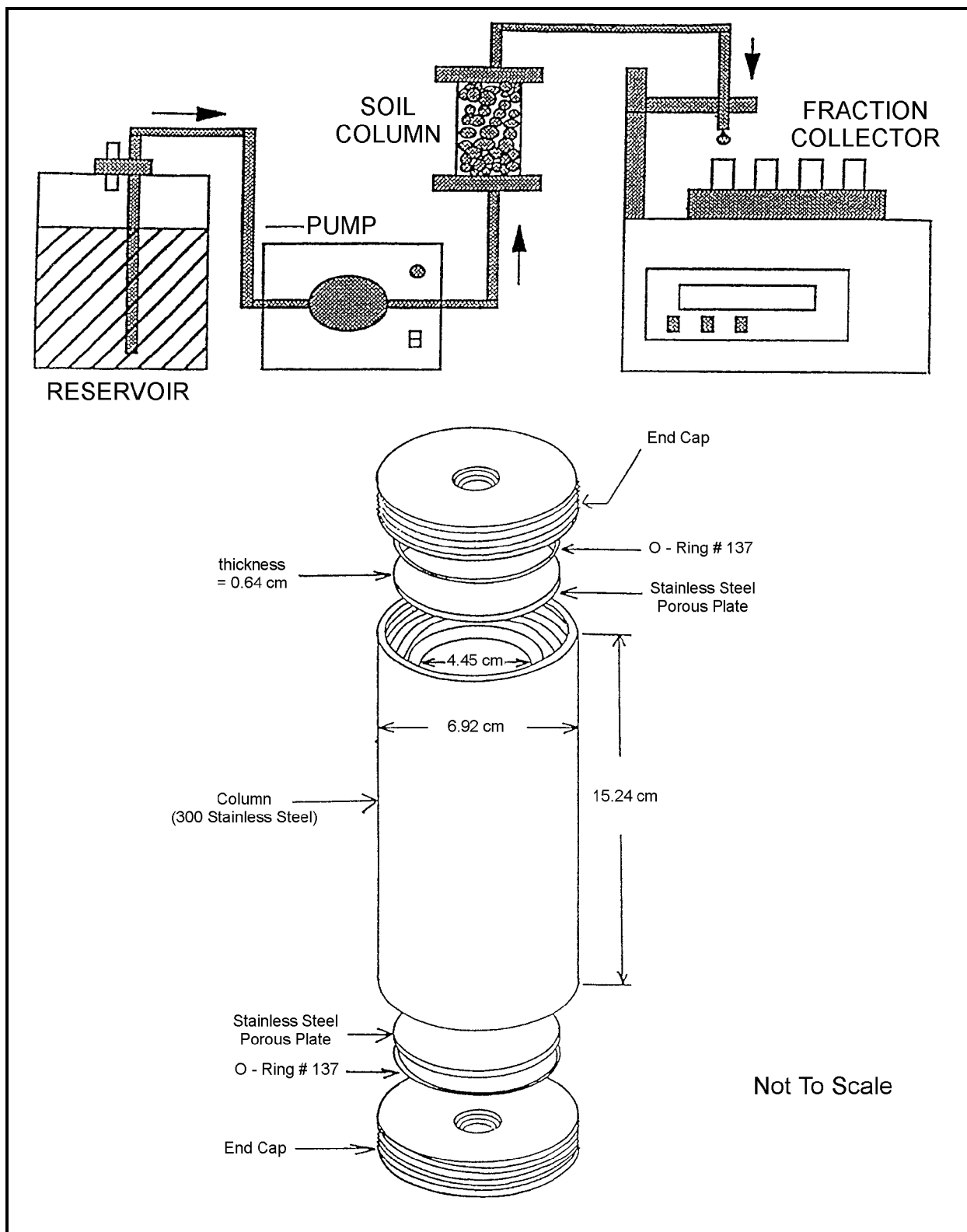


Figure 2. Soil column test apparatus and soil column schematic

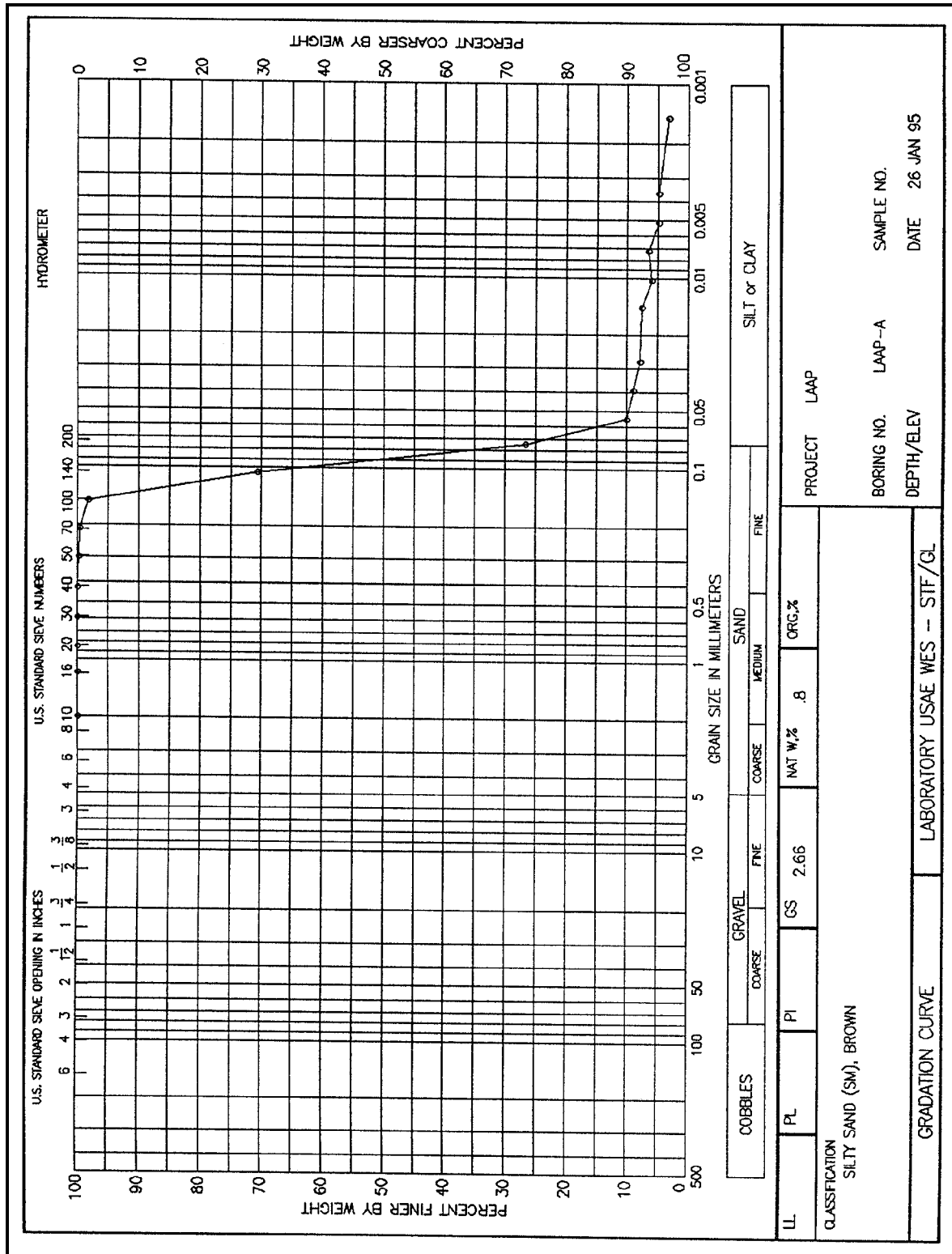


Figure 3. Soil A particle size distribution

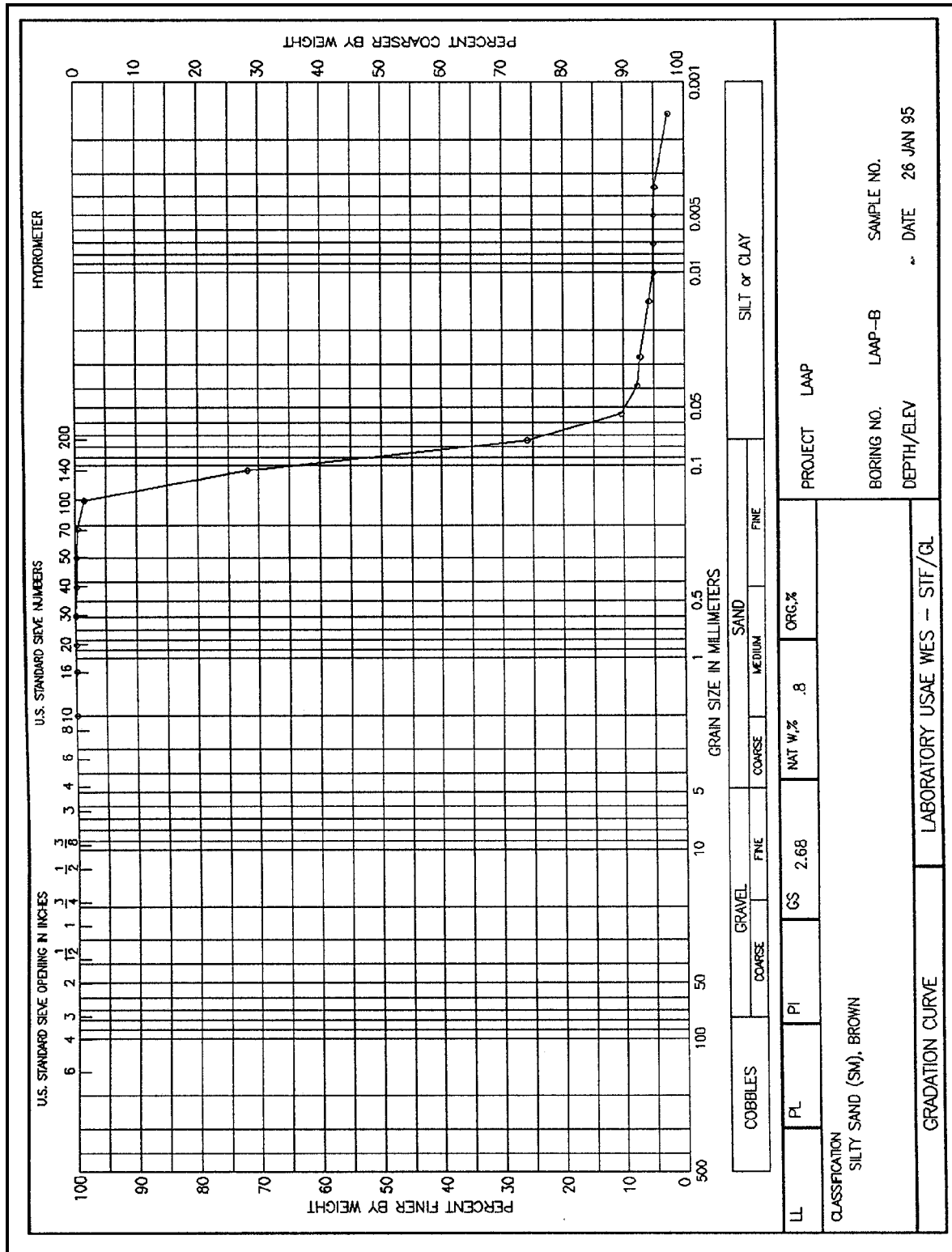


Figure 4. Soil B particle size distribution

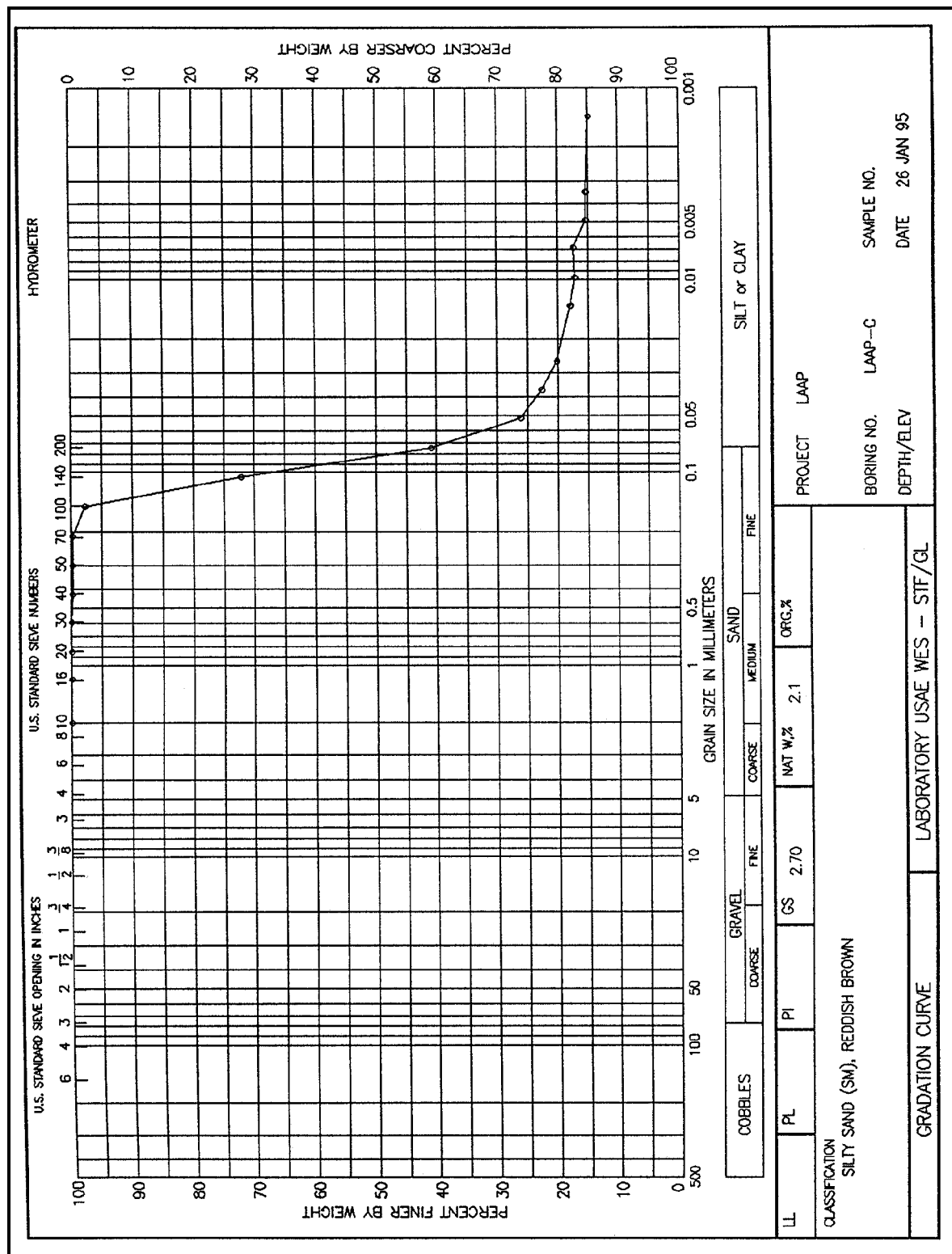


Figure 5. Soil C particle size distribution

Table 2
Column Operating Parameters

Soil	A	B	C	D
Bulk Density, g/cm ³	1.15	1.23	1.13	1.14
Effective Porosity	0.53	0.49	0.45	0.46
Average Pore Water Velocity, cm/sec	1.3×10^{-4}	1.4×10^{-4}	1.8×10^{-4}	1.1×10^{-4}

After loading the columns with soil, uncontaminated water was prepared using groundwater from Ada, OK, with a pH of 7.56, a conductivity of 645 μ S, and an alkalinity (as CaCO₃) of 420 mg/ℓ and de-aired, distilled deionized (DDI) water at a ratio of one part groundwater to two parts DDI water. Uncontaminated water was pumped at steady flow through the columns for approximately 3 weeks in order to allow the hydraulic properties of the columns to stabilize. TNT-contaminated water was prepared by dissolving 10-percent hydrated TNT (Eastman Kodak, Rochester, NY) in de-aired DDI water and mixing with the groundwater discussed previously at a ratio of one part groundwater to two parts TNT solution. TNT-contaminated water was then pumped into the columns at steady flow to provide a step input loading sufficient to displace approximately 9 to 13 pore volumes. Concentrations of TNT, 2-amino-4,6-dinitrotoluene (2A-DNT), 4-amino-2,6-dinitrotoluene (4A-DNT), 2,4-diamino-6-nitrotoluene (2,4-DANT), 2,6-diamino-4-nitrotoluene (2,6-DANT), 1,3,5-trinitrobenzene (TNB), 1,3-dinitrobenzene (DNB), 2,6-dinitrotoluene (2,6-DNT), 2,4-dinitrotoluene (2,4-DNT), 4,4',6,6'-tetranitro-2,2'-azoxytoluene (2,2-AZOX), and 2,2', 6,6'-tetranitro-4,4'-azoxytoluene (4,4-AZOX) in the TNT-contaminated groundwater were monitored throughout the experiment (Table 3). After step input loading of the TNT-contaminated groundwater, columns were eluted with uncontaminated water at the same flow used for the step input loading.

Table 3
Step Input Contaminant Concentrations, mg/ℓ

Day	TNT	2A-DNT	4A-DNT	2,4-DANT	2,6-DANT	TNB	DNB	2,6-DNT	2,4-DNT	2,2-AZOX	4,4-AZOX
0	42.7	0.010 J ¹	<0.020	<0.200	<0.100	0.013	<0.020	<0.020	0.071	<0.500	<0.500
3	46.5	0.012 J	<0.020	<0.200	<0.100	0.019	<0.020	<0.020	0.078	<0.500	<0.500
6	46.6	0.013 J	<0.020	<0.200	<0.100	0.024	<0.020	<0.020	0.078	<0.500	<0.500
9	46.1	<0.020	0.011 J	<0.200	<0.100	0.031	<0.020	<0.020	0.077	<0.500	<0.500
12	46.4	<0.020	0.012 J	<0.200	<0.100	0.033	<0.020	<0.020	0.077	<0.500	<0.500
15	46.9	0.014 J	0.023	<0.200	<0.100	0.044	<0.020	<0.020	0.076	<0.500	<0.500

¹ J indicates an estimated value between the method detection limit and the laboratory reporting limit.

At the end of the column elution experiments, the soils were extruded, sectioned, and analyzed for TNT, 2A-DNT, 4A-DNT, 2,4-DANT, 2,6-DANT, TNB, DNB, 2,6-DNT, 2,4-DNT, and 2,2-AZOX using two high performance liquid chromatography (HPLC) systems as described in the following section.

Explosives analysis

Column eluate samples were collected in approximately 15-ml increments in amber glass vials (20-ml) using automated fraction collectors (Model UFC, Eldex Laboratories, Napa, CA). Aliquots of each sample were preserved with an equal amount of acetonitrile within 24 hr of collection and stored at 4 °C in capped vials until analyzed. Soil column eluate samples were analyzed by HPLC for TNT, 2A-DNT, 4A-DNT, 2,4-DANT, 2,6-DANT, TNB, DNB, 2,6-DNT, and 2,4-DNT using the dual column confirmation method developed by Jenkins, Miyares, and Walsh (1988). Sample extracts were filtered through a 0.5- μ m polytetrafluoroethylene filter and analyzed independently on two HPLC systems (Waters Chromatography Division, Milford, MA). The first HPLC system consisted of a 600 system controller, a 717plus Autosampler, and a 486 Tunable Absorbance Detector. The second HPLC system consisted of an LC Module I. The column for the first system was a Supelcosil LC-18 HPLC column (25 cm by 4.6 mm, Supelco, Bellefonte, PA) eluted with 1:1 methanol/water at 1.2 ml/min. The column for the second system was an HPLC-CN (Supelco 25 cm by 4.6 mm) column eluted with 1:1 methanol/water at 1.2 ml/min. Soil column eluate samples were analyzed for 2,2-AZOX and 4,4-AZOX on a Waters 2690 Alliance Separations Module using a Waters 996 Photodiode Array Detector. The column was a Waters Nova-Pak C18 column (3.9 by 150 mm) eluted with 54:46 acetonitrile/water at 1.5 ml/min.

Sectioned samples from each soil column were analyzed using the procedure developed by Jenkins and Walsh (1987). A portion of each sectioned soil sample (3 g) was extracted for 18 hr in a sonic bath with 10 ml of acetonitrile. The extracts were diluted 1:1 with calcium chloride solution (5 g/l), filtered through a 0.5- μ m polytetrafluoroethylene filter, and analyzed on the HPLC systems previously described.

Dispersion coefficients

Following the elution of explosives, column dispersion coefficients were determined using a chloride tracer. A constant input of sodium chloride solution at approximately 105 mg/l as Cl⁻ was pumped into the columns until the input Cl⁻ concentration was achieved in the effluents. Chloride concentrations in column eluates were measured potentiometrically using a chloride selective ion electrode (Orion 9417B) in conjunction with a double junction, sleeve-type reference electrode (Orion 90-02). Potentials were measured on an ion-selective meter (Orion 720A). Nonlinear curve fitting (Tablecurve, Jandel Scientific, Corte Madera, CA) was used to estimate dispersion coefficients by fitting the semi-infinite model for constant input (van Genuchten and Alves 1982) to the chloride elution curves. The semi-infinite model for constant input is given in Equation 1.

$$C_T = \frac{C_0}{2} \left[\operatorname{erfc} \left(\frac{(1 - T)L}{2 \left(\frac{DTL}{u} \right)^{\frac{1}{2}}} \right) + \exp \left(\frac{uL}{D} \right) \operatorname{erfc} \left(\frac{(1 + T)L}{2 \left(\frac{DTL}{u} \right)^{\frac{1}{2}}} \right) \right] \quad (1)$$

where

C_T = chloride concentration at L and T , $\text{mg } \ell^{-1}$

C_o = constant input chloride concentration, $\text{mg } \ell^{-1}$

T = pore volumes eluted, dimensionless

L = column length, cm

D = dispersion coefficient, $\text{cm}^2 \text{ sec}^{-1}$

u = average pore water velocity, cm sec^{-1}

The average pore water velocity (u) is calculated from Equation 2,

$$u = \frac{Q}{A\theta_e} \quad (2)$$

where

Q = average flow, $\text{cm}^3 \text{ sec}^{-1}$

A = cross-sectional area of column, cm^2

θ_e = effective porosity, dimensionless

The number of pore volumes eluted (T) is calculated from Equation 3,

$$T = \frac{ut}{L} \quad (3)$$

where t equals time, sec .

In almost all cases, the second term in Equation 1 is negligible (Domenico and Schwartz 1990). Thus, for a constant input of conservative tracer, the effluent tracer concentration equals approximately one-half of the input concentration ($C/C_o = 0.5$) when approximately one pore volume has been eluted ($T = 1$) since the complementary error function of zero is one. Since the average flow, cross-sectional area of column, and column length are known (from column operating records and column dimensions), and time at $C/C_o = 0.5$ is known (from column operating records), the effective porosity was calculated for each column from Equations 2 and 3. The calculated effective porosities were then used to calculate average pore water velocities, which in turn were used to calculate the number of pore volumes eluted for each collected sample.

Figure 7 shows the observed and fitted chloride elution curves for each soil column. From nonlinear curvefitting of Equation 1 to chloride elution curves, dispersion coefficients of $4.4 \times 10^{-5} \text{ cm}^2/\text{sec}$, $3.0 \times 10^{-5} \text{ cm}^2/\text{sec}$,

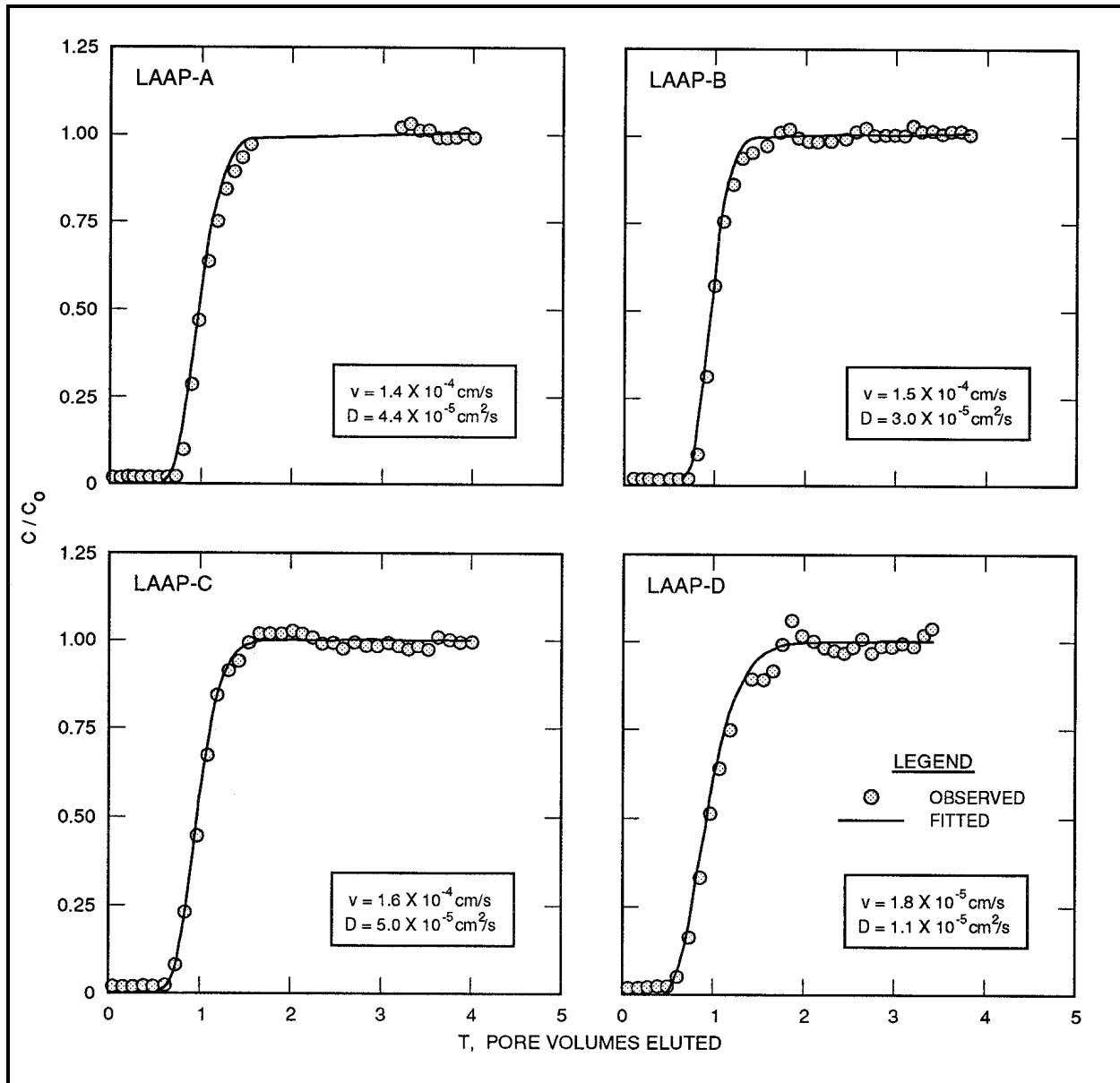


Figure 7. Observed and fitted chloride elution curves

$5.0 \times 10^{-5} \text{ cm}^2/\text{sec}$, and $1.1 \times 10^{-5} \text{ cm}^2/\text{sec}$ were obtained for Soils A, B, C, and D, respectively.

Semianalytical Model

TNT breakthrough curves were simulated using the semianalytical model developed by Moldrup et al. (1992) and Yamaguchi et al. (1994) for solute transport in soils. The Moldrup et al. (1992) and Yamaguchi et al. (1994) model incorporates linear or nonlinear reaction terms into the one-dimensional advection-dispersion equation for solute transport and is based on the Moving

Concentration Slope (MCS) solute transport model developed in Moldrup et al. (1992). In the MCS model, an integrated version of the solute flux equation is used together with a simple, forward-time discretization (Moldrup et al. 1992).

Model description

The following description was condensed from the model development provided by Yamaguchi et al. (1994) and Moldrup et al. (1992). For steady water flow, the governing flux and continuity equations are described by Equations 4 and 5, respectively,

$$J = -D \frac{C}{Z} + uC \quad (4)$$

$$\frac{C}{t} = -\frac{J}{Z} - S \quad (5)$$

where

J = contaminant flux, cm mg sec⁻¹ ℓ⁻¹

D = dispersion coefficient, cm² sec⁻¹

C = liquid phase contaminant concentration, mg ℓ⁻¹

Z = distance from column inlet, cm

t = time, sec

S = contaminant removal rate, mg ℓ⁻¹ sec⁻¹

For sorption and first-order decay,

$$S = \frac{\rho_b}{\theta} \frac{\bar{C}}{t} + \mu C \quad (6)$$

where

D_b = bulk density, kg ℓ⁻¹

\bar{C} = solid phase contaminant concentration, mg kg⁻¹

θ = porosity, dimensionless

μ = first-order contaminant decay rate coefficient, sec⁻¹

Applying the chain rule (Equation 7), substituting into Equation 6, and rearranging, Equation 8 is obtained,

$$\frac{\bar{C}}{t} = \frac{\bar{C}}{C} \frac{C}{t} \quad (7)$$

$$\left(1 + \frac{\rho_b}{\theta} \frac{\bar{C}}{C} \right) \frac{C}{t} = \left(-\frac{J}{Z} - \mu C \right) \quad (8)$$

where the term in parentheses on the left-hand side of Equation 8 is the generalized form of the retardation factor, R

$$R = \left(1 + \frac{\rho_b}{\theta} \frac{\bar{C}}{C} \right) \quad (9)$$

A forward-time discretization of Equation 8 yields Equation 10.

$$C_Z^{t+\Delta t} = C_Z^t + \frac{1}{R} \left(J_{Z+\frac{1}{2}\Delta Z}^t - J_{Z-\frac{1}{2}\Delta Z}^t \right) \frac{\Delta t}{\Delta Z} - \frac{1}{R} \mu C_Z^t \Delta t \quad (10)$$

where subscript Z denotes distance from the column inlet and superscript t denotes time. For instance, $J_{z+1/2\Delta z}^t$ is the contaminant flux at time t at a distance from the column inlet halfway between Z and ΔZ .

From Yamaguchi et al. (1994),

$$J_{Z+\frac{1}{2}\Delta Z}^t = - \left(\frac{u}{e^{(u\Delta Z)/2} - 1} - \frac{D_{num}}{\Delta Z} \right) (C_{Z+\frac{1}{2}\Delta Z}^t - C_Z^t) + u C_Z^t \quad (11)$$

and

$$D_{num} = u \frac{\Delta Z}{2} - u^2 \frac{\Delta t}{2} + \frac{u \Delta Z}{e^{(u\Delta Z)/2} - 1} - D \quad (12)$$

where

D_{num} = numerical dispersion coefficient ($\text{cm}^2 \text{sec}^{-1}$), which corrects the model for the artificial dispersion created by the calculation scheme itself

Δt = time increment, sec

ΔZ = distance increment used in the calculations, cm

To enable the derivation of a closed-form solution, Yamaguchi et al. (1994) approximated the contaminant flux at $Z = 0$ using ΔZ , rather than one-half ΔZ as in the Moldrup et al. (1992) MCS model. Yamaguchi et al. (1994) suggest that no significant errors are introduced by this approximation compared with the flux approximation of Moldrup et al. (1992) provided ΔZ is chosen to be less than or equal to 0.5.

Introducing the solute unit mean travel distance (Φ) and the solute dispersivity (β),

$$\Phi = u\Delta t \quad (13)$$

$$\beta = \frac{D}{u} \quad (14)$$

and substituting Equations 11, 12, 13, and 14 into Equation 10, Equation 15 is obtained.

$$\begin{aligned} C_Z^{t+\Delta t} = & \frac{1}{R} \left(\frac{-\Phi^2}{\Delta Z^2} - 2\frac{\beta\Phi}{\Delta Z^2} + R \right) C_Z^t \\ & + \frac{1}{R} \left(\frac{\Phi}{2\Delta Z} + \frac{\Phi^2}{2\Delta Z^2} + \frac{\beta\Phi}{\Delta Z^2} \right) C_{Z+\Delta Z}^t \\ & + \frac{1}{R} \left(\frac{-\Phi}{2\Delta Z} + \frac{\Phi^2}{2\Delta Z^2} - \frac{\beta\Phi}{\Delta Z^2} \right) C_{Z-\Delta Z}^t \\ & - \frac{1}{R} \mu C_Z^t \Delta t \end{aligned} \quad (15)$$

Equation 15 represents the semianalytical solution for solute transport with equilibrium sorption and first-order decay. In order to avoid stability problems, the maximum distance (Z_{max}) to be used in the calculation scheme should be chosen using the following criteria (Yamaguchi et al. 1994),

$$Z_{max} > \left(2 + \frac{D}{u} \right) I_{max} \mu \Delta t \quad (16)$$

where I_{max} equals the maximum number of time steps, and the value of Φ chosen should meet the following three stability criteria (Yamaguchi et al. 1994),

$$\Phi < 0.5 \frac{e^{0.5\beta} - 1}{e^{0.5\beta} + 1} \quad (17)$$

$$\Phi < 0.15 \quad (18)$$

$$-2 < \frac{1}{\beta} \left(0.25 + \frac{0.5}{e^{0.5\beta} - 1} \right) - \frac{1}{\beta} (0.5\Phi + \beta) < 2 \quad (19)$$

Sorption descriptors

Any number of equilibrium sorption models may be used simply by defining M/C in the retardation factor (Equation 9).

For linear sorption,

$$\frac{\bar{C}}{C} = K_d \quad (20)$$

where K_d equals the linear equilibrium distribution coefficient, $\ell \text{ kg}^{-1}$.

Thus, for linear sorption, $R = 1 + D_b K_d / 2$.

For the Freundlich sorption isotherm,

$$\frac{\bar{C}}{C} = n K_f (C_z)^{n-1} \quad (21)$$

where

n = empirical constant

K_f = Freundlich constant, $\text{mg}^{(1-n)} \ell^n \text{ kg}^{-1}$

For the Langmuir sorption isotherm,

$$\frac{\bar{C}}{C} = \frac{K_1 Q}{(1 + K_1 C_z)^2} \quad (22)$$

where

K_1 = Langmuir constant, $\ell \text{ mg}^{-1}$

Q = sorption capacity, mg kg^{-1}

Equation 15 may also be adapted for nonequilibrium sorption formulations, as well as decay terms other than first-order. For the film diffusion physical nonequilibrium sorption model (adapted from the general mass transfer isotherm given in McGrath 1995),

$$\frac{\bar{C}}{t} = K_{film} (C - C^*) \quad (23)$$

where

K_{film} = film coefficient, $\ell \text{ kg}^{-1} \text{ t}^{-1}$

C^* = contaminant concentration in film immediately adjacent to solid particle, $\text{mg } \ell^{-1}$

The film diffusion model views transport of contaminants through a film surrounding the sorbate as a rate-limiting process. The actual adsorption and desorption processes may still be equilibrium processes. Thus, for the case of film diffusion with equilibrium sorption and first-order decay, the film diffusion term is added to Equation 6, to yield Equation 24

$$S = \left(\frac{\rho_b}{\theta} K_{film} C - C^* \right) + \mu C \quad (24)$$

and

$$\begin{aligned} C_z^{(t)} = & \frac{1}{R} \left(\frac{-\Phi^2}{\Delta Z^2} - 2 \frac{\beta \Phi}{\Delta Z^2} + R \right) C_z^t \\ & + \frac{1}{R} \left(\frac{\Phi}{2\Delta Z} + \frac{\Phi^2}{2\Delta Z^2} + \frac{\beta \Phi}{\Delta Z^2} \right) C_{z+\Delta z}^t \\ & + \frac{1}{R} \left(\frac{-\Phi}{2\Delta Z} + \frac{\Phi^2}{2\Delta Z^2} + \frac{\beta \Phi}{\Delta Z^2} \right) C_{z-\Delta z}^t \\ & - \frac{1}{R} \left(\mu C_z^t + K_{film} C_z^t + K_{film} C^* \right) \Delta t \end{aligned} \quad (25)$$

The film diffusion model can also be used to describe contaminant dissolution. For contaminant dissolution, C^* is defined as the contaminant concentration in the film immediately adjacent to the contaminant crystal and is equal to the aqueous solubility limit for the contaminant. Ro et al. (1996) report a range of 100 to 110 mg/ℓ for the aqueous solubility limit of TNT at 25 °C.

Thus, sorption formulations other than linear equilibrium may be investigated and applied to column data using the semianalytical contaminant transport model. Transformation formulations other than first-order (not shown here) may also be incorporated into the model by modifying the last term (μC_z^t) in Equation 25.

3 Results and Discussion

Results

Model testing

The Moldrup et al. (1992) and Yamaguchi et al. (1994) semianalytical model was implemented using the software program MathCAD (MathSoft, Inc.). An example of the MathCAD implementations used in this report for the semianalytical model is shown in Appendix A. In this example, semianalytical model results are fitted to observed data for a single BTC. The semianalytical model was compared with the analytical model of Cleary and Adrian (1973), an analytical model from Bear (1972), and the numerical model of Grove and Stollenwerk (1984).

The Cleary-Adrian analytical model incorporates linear equilibrium sorption into the advection-dispersion equation. Figure 8 shows a comparison of the semianalytical model to the Cleary-Adrian model. Nearly identical results were obtained from each model for a variety of linear equilibrium distribution coefficients (K_d).

The model from Bear (1972) that was compared with the semianalytical model (Figure 9) is an analytical solution with linear equilibrium sorption along with terms for first-order decay (μ) and zero-order growth (γ). In this comparison, the ratio of the zero-order growth term (γ) to the first-order decay term (μ) were varied from 0.1 to 1.0. Excellent agreement between the semianalytical model and the Bear model were obtained.

The Grove-Stollenwerk numerical model is capable of nonlinear sorption and/or decay terms. Figure 10 shows a comparison between the semianalytical model and the Grove-Stollenwerk model for various values of the empirical coefficient (n) in the Freundlich sorption term. The two models compared well, although differences in the results from the two models increased slightly as values of the empirical coefficient decreased. A comparison between the semianalytical model and the Grove-Stollenwerk model for Langmuir equilibrium sorption was also conducted (Figure 11). The two models compared well for a large range of input concentrations.

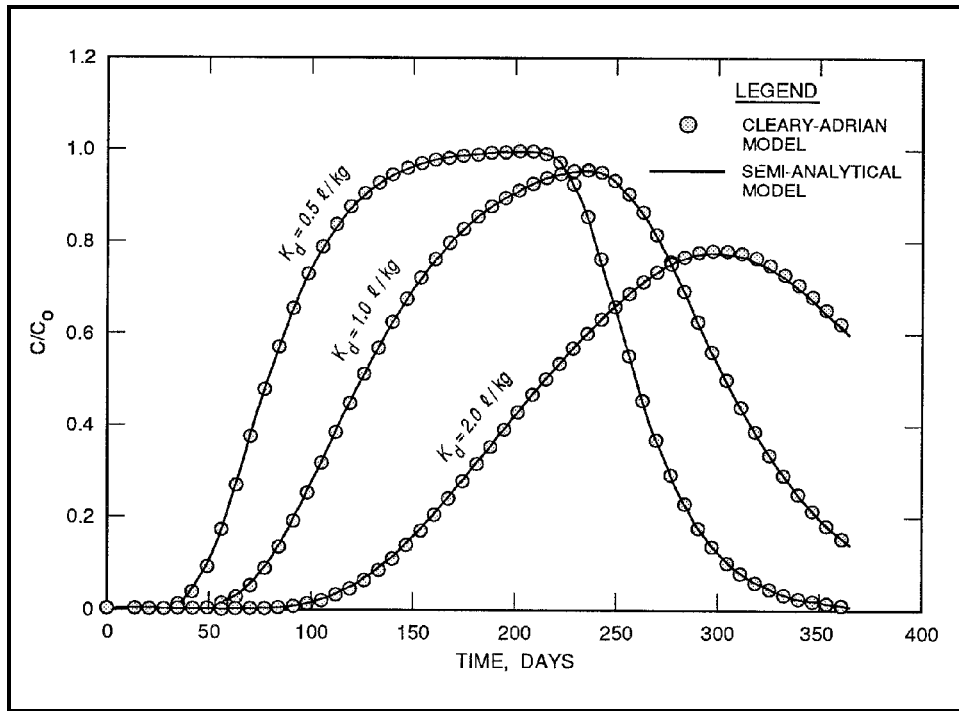


Figure 8. Comparison of the semianalytical solution to the analytical solution of Cleary and Adrian (1973)

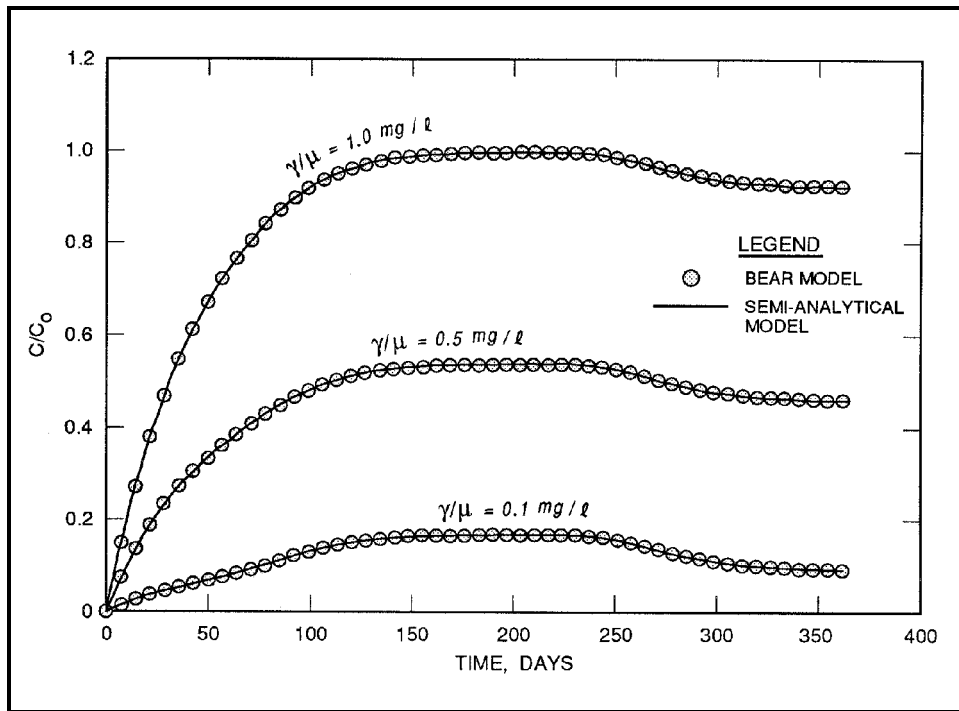


Figure 9. Comparison of the semianalytical solution to an analytical solution from Bear (1972)

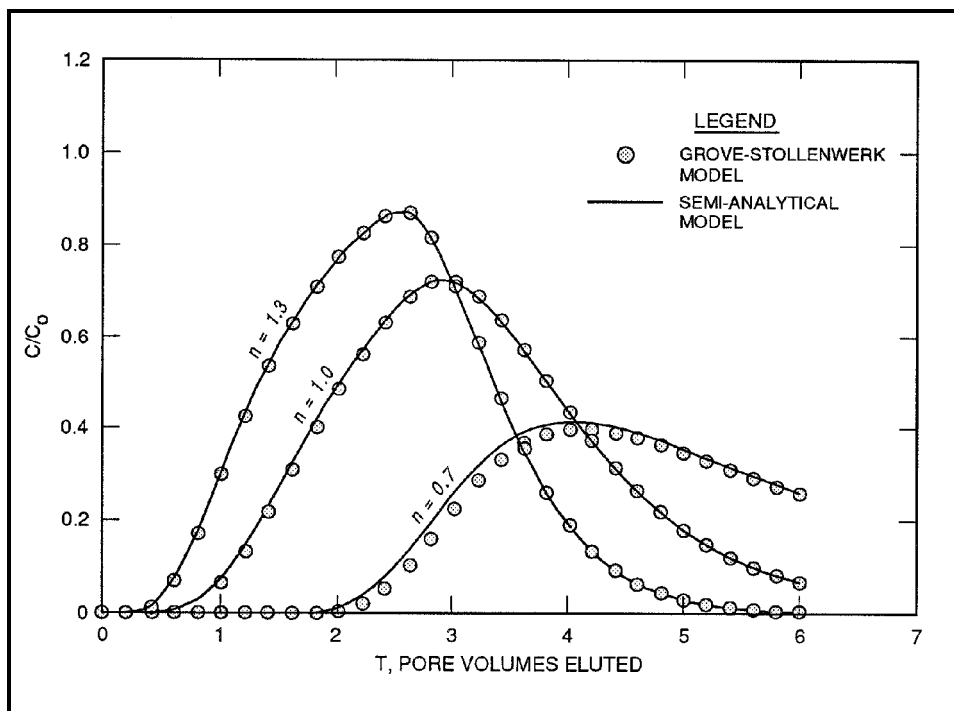


Figure 10. Comparison of the semianalytical solution to the numerical model of Grove and Stollenwerk (1984) for Freundlich sorption

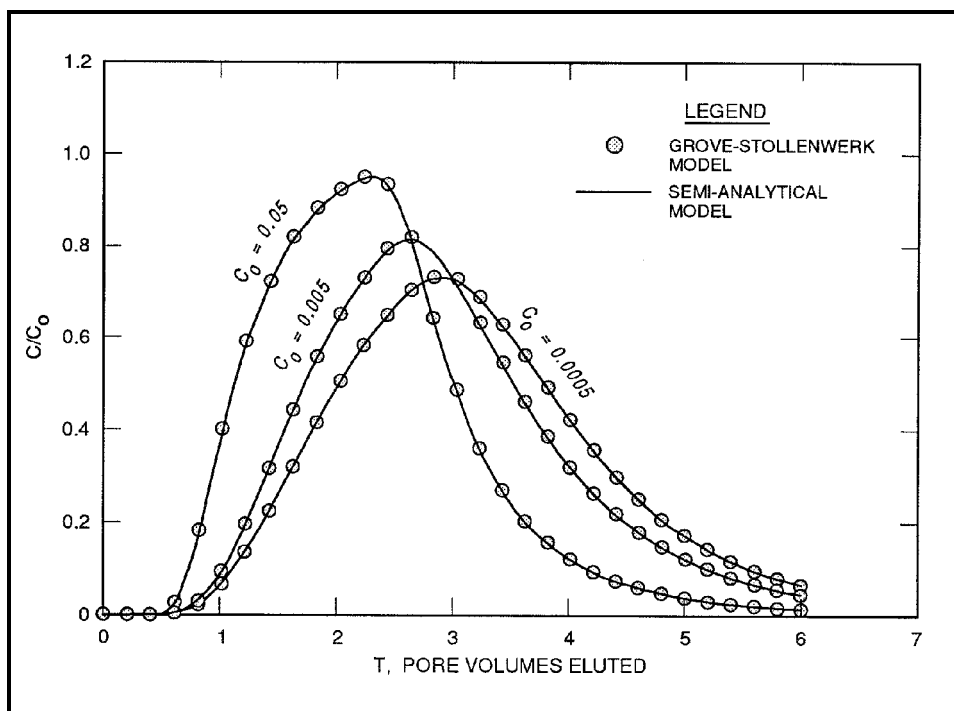


Figure 11. Comparison of the semianalytical solution to the numerical model of Grove and Stollenwerk (1984) for Langmuir sorption

TNT transport modeling considerations

The semianalytical model was fitted to the TNT BTCs from Soils A through D. Various process descriptors were evaluated for applicability to the data.

The semianalytical model was also applied to a TNT leaching curve for a field-contaminated soil (Crane soil) reported elsewhere (Pennington et al. 1995). Crane soil was obtained from the Naval Weapons Support Center, Crane, IN, and contained a TNT concentration of approximately 25.8 mg/kg (Pennington et al. 1995).

The goodness of fits of the model to the data were quantified using the Root Mean Square (Equation 26).

$$RMS = \sqrt{\frac{\sum_{i=1}^N (C_{fit} - C_{obs})^2}{N - F}} \quad (26)$$

where

RMS = root mean square value, $\text{mg } \ell^{-1}$

C_{fit} = theoretical contaminant effluent concentration, $\text{mg } \ell^{-1}$

C_{obs} = observed contaminant effluent concentration, $\text{mg } \ell^{-1}$

N = number of data points

F = number of adjustable parameters used to fit model to observed data

Each TNT BTC reached a steady-state effluent TNT concentration. At steady state, the rates of adsorption and desorption are equal, and thus are eliminated from the advection-dispersion model. For first-order decay, the steady-state effluent TNT concentration (C_{ss}) is calculated from Equation 27 (van Genuchten and Alves 1982)

$$C_{ss} = C_0 \exp\left[\frac{(u - v) z}{2D}\right] \quad (27)$$

where C_{ss} equals the steady-state effluent contaminant concentration, $\text{mg } \ell^{-1}$, and where v is calculated from the following

$$v = u \left(1 + \frac{4\mu D}{u^2} \right)^{\frac{1}{2}} \quad (28)$$

Combining Equations 27 and 28, and rearranging, the first-order transformation rate constant (μ) is solved for (Equation 29)

$$\mu = \ln\left(\frac{C_{ss}}{C_o}\right) \left[-\frac{u}{z} + \frac{D}{z^2} \ln\left(\frac{C_{ss}}{C_o}\right) \right] \quad (29)$$

Thus, first-order transformation rate constants were calculated from the steady-state portion of the TNT BTCs, leaving only the parameter(s) for sorption to be obtained from the semianalytical model fits. TNT BTCs for Soils A, B, C, and D were evaluated using first-order transformation with linear, Freundlich, and Langmuir equilibrium sorption formulations.

The TNT elution curve for Crane soil was evaluated using first-order transformation with linear, Freundlich, and Langmuir equilibrium sorption formulations. A descriptor for dissolution (diffusion-limited mass transfer) was also incorporated into the semianalytical model and applied to the Crane elution curve.

Equation 29 does not apply to the Crane soil elution curve. Thus, a first-order TNT transformation rate constant for the Crane soil could not be obtained without fitting a model to the elution data. Furthermore, multiple combinations of sorption and transformation parameters provided essentially identical fits when sorption and transformation were the only processes modeled. When dissolution was added to the processes modeled, however, a single first-order transformation rate constant was obtained. This constant was used in the Crane elution curve fits where sorption and transformation were the only processes modeled.

Soil A. Figure 12 shows the observed TNT BTC for Soil A and the fitted semianalytical model results for linear equilibrium sorption and first-order transformation. A first-order transformation rate constant (μ) of 0.0011 hr^{-1} , obtained from the steady-state portion of the BTC, was used in the semianalytical model. Linear equilibrium sorption, along with first-order transformation, provided an adequate fit to the Soil A TNT BTC ($RMS = 1.856 \text{ mg } \ell^{-1}$). Near the end of wash-out, the Soil A TNT BTC shows a small amount of tailing, which could not be captured using linear equilibrium sorption and first-order transformation. A linear equilibrium distribution coefficient (K_d) of $0.12 \text{ } \ell/\text{kg}$ was obtained for the Soil A TNT BTC.

Figure 13 shows the observed TNT BTC for Soil A and the fitted semianalytical model results for Freundlich equilibrium sorption and first-order transformation. Freundlich equilibrium sorption improved the fit ($RMS = 1.775 \text{ mg } \ell^{-1}$) over the fit provided by the linear sorption model. Improvement of the fit was due primarily to the ability of the Freundlich model to capture the slight tailing observed in the BTC. A Freundlich constant (K_f) of $0.45 \text{ mg}^{(1-n)} \ell^n \text{ kg}^{-1}$ and an empirical coefficient (n) of 0.73 were obtained.

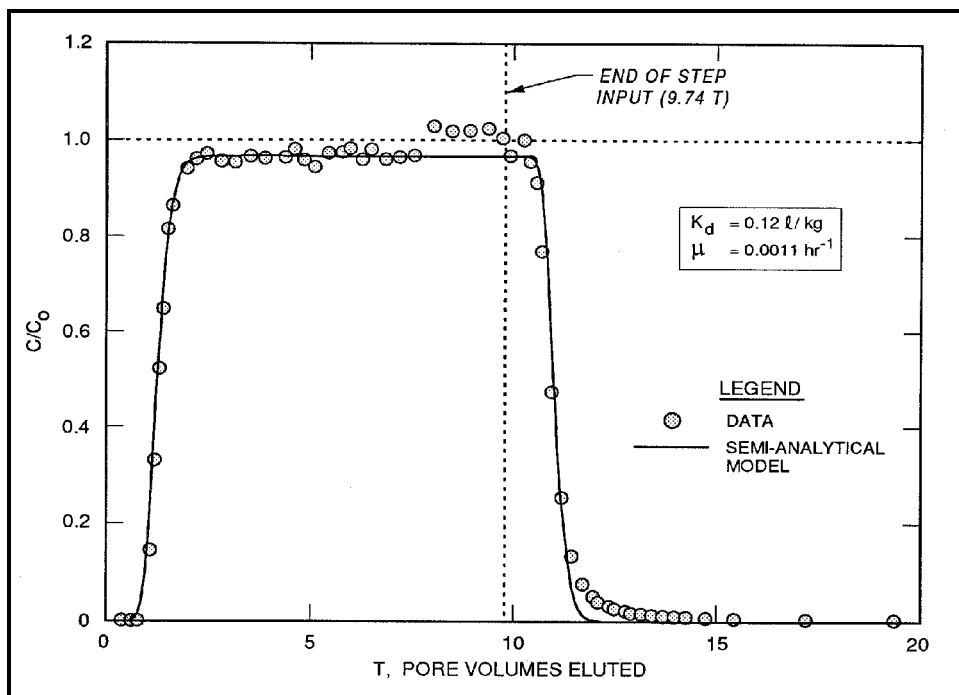


Figure 12. Observed and fitted TNT breakthrough curves for Soil A for linear sorption and first-order transformation

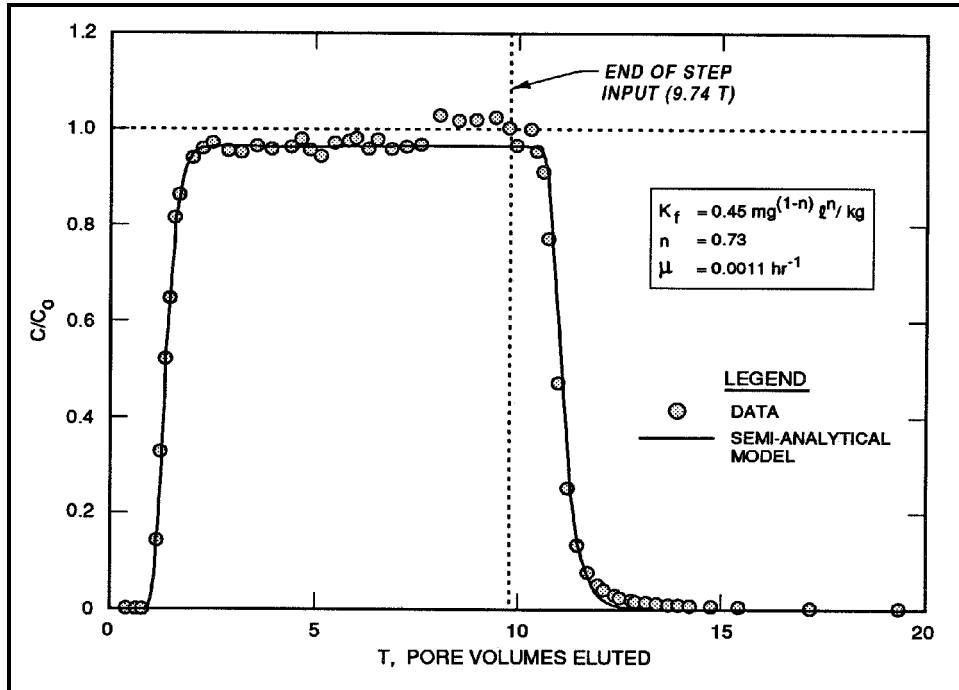


Figure 13. Observed and fitted TNT breakthrough curves for Soil A for Freundlich sorption and first-order transformation

Figure 14 shows the observed TNT BTC for Soil A and the fitted semianalytical model results for Langmuir equilibrium sorption and first-order transformation. Langmuir equilibrium sorption improved the fit ($RMS = 1.265 \text{ mg } \ell^{-1}$) over the fits provided by the linear and Freundlich sorption models. The Langmuir sorption model, like the Freundlich model, was able to capture most of the tailing shown by the Soil A TNT BTC. A Langmuir constant (K_1) of $0.04 \text{ } \ell/\text{mg}$ and a sorption capacity (Q) of 9.0 mg/kg were obtained.

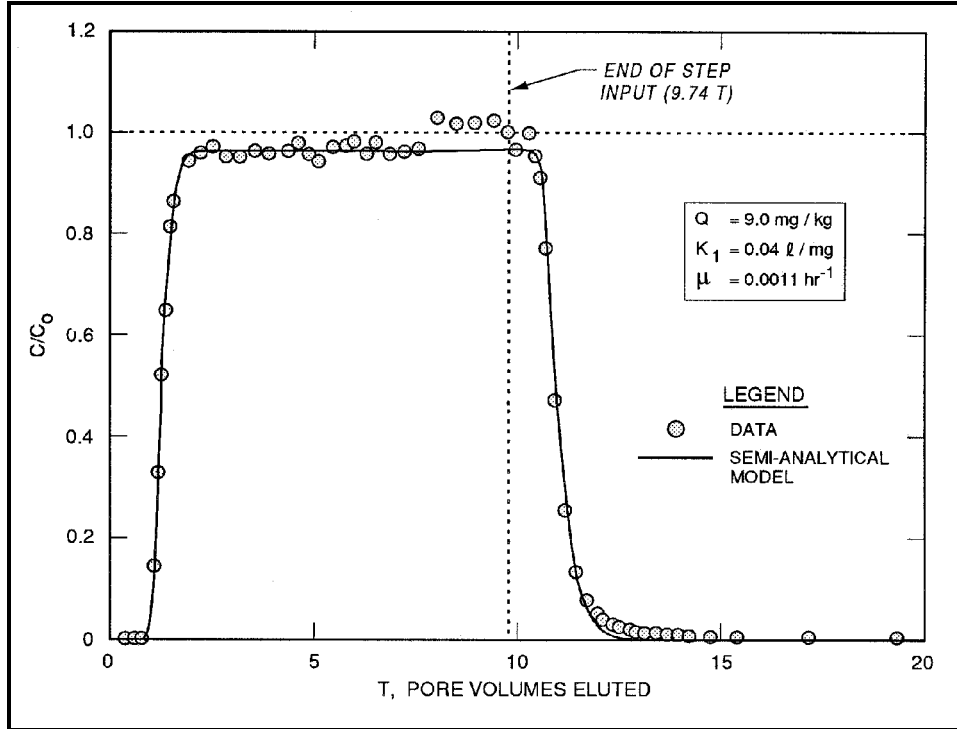


Figure 14. Observed and fitted TNT breakthrough curves for Soil A for Langmuir sorption and first-order transformation

Soil B. Figure 15 shows the observed TNT BTC for Soil B and the fitted semianalytical model results for linear equilibrium sorption. Since steady-state TNT effluent concentrations were at the step input TNT concentration, transformation was negligible during transport through Soil B. Linear equilibrium sorption provided an adequate fit to the Soil B TNT BTC ($RMS = 2.973 \text{ mg } \ell^{-1}$). Near the end of washout, the Soil B TNT BTC shows a small amount of tailing, like the Soil A TNT BTC, which could not be captured using linear equilibrium sorption. A linear equilibrium distribution coefficient (K_d) of $0.11 \text{ } \ell/\text{kg}$ was obtained for the Soil B TNT BTC.

Figure 16 shows the observed TNT BTC for Soil B and the fitted semianalytical model results for Freundlich equilibrium sorption. Freundlich equilibrium sorption improved the fit ($RMS = 2.199 \text{ mg } \ell^{-1}$) slightly over the fit provided by the linear sorption model. Improvement of the fit was due primarily to the ability of the Freundlich model to capture the slight tailing observed in the BTC, as with

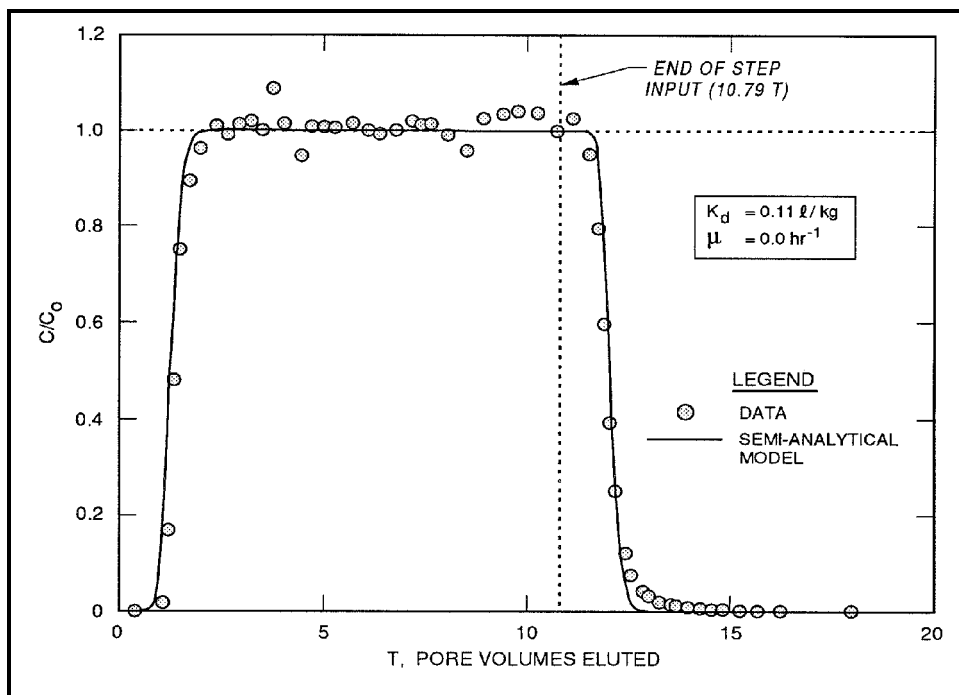


Figure 15. Observed and fitted TNT breakthrough curves for Soil B for linear sorption and first-order transformation

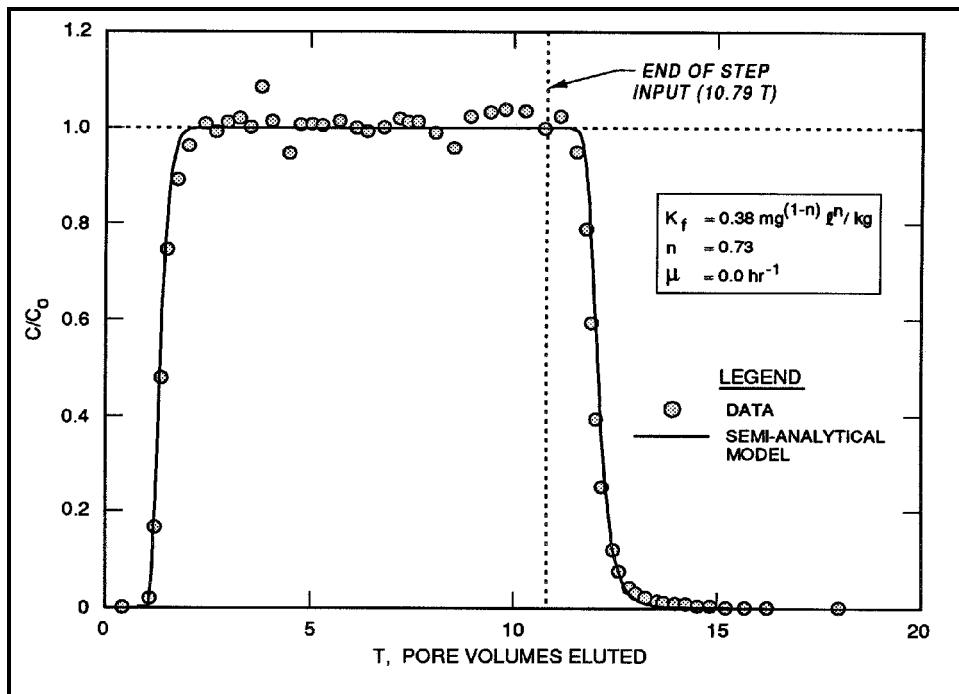


Figure 16. Observed and fitted TNT breakthrough curves for Soil B for Freundlich sorption and first-order transformation

Soil A. A Freundlich constant (K_f) of $0.38 \text{ l}^n/\text{kg}^n$ and an empirical coefficient (n) of 0.73 were obtained.

Figure 17 shows the observed TNT BTC for Soil B and the fitted semianalytical model results for Langmuir equilibrium sorption. Langmuir equilibrium sorption improved the fit ($RMS = 1.857 \text{ mg l}^{-1}$) slightly over the fits provided by the linear and Freundlich sorption models. The Langmuir sorption model, like the Freundlich model, was able to capture most of the tailing shown by the Soil B TNT BTC. A Langmuir constant (K_1) of 0.045 l/mg and a sorption capacity (Q) of 9.0 mg/kg were obtained.

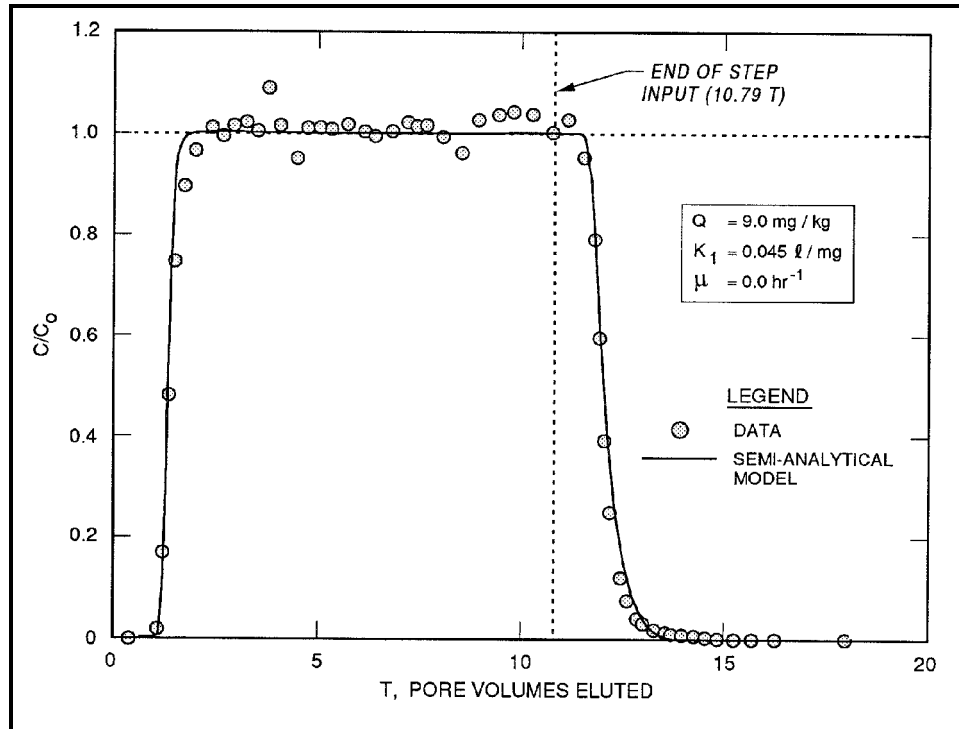


Figure 17. Observed and fitted TNT breakthrough curves for Soil B for Langmuir sorption and first-order transformation

Soil C. Figure 18 shows the observed TNT BTC for Soil C and the fitted semianalytical model results for linear equilibrium sorption. Like the TNT BTC for Soil B, steady-state TNT effluent concentrations were at the step input TNT concentration, indicating that transformation during transport through Soil C soil was negligible. Linear equilibrium sorption provided an adequate fit to most of the Soil C TNT BTC ($RMS = 3.214 \text{ mg l}^{-1}$). Near the end of washout, the Soil C TNT BTC showed tailing, which could not be captured using the model with linear equilibrium sorption. A linear equilibrium distribution coefficient (K_d) of 0.47 l/kg was obtained for the Soil C TNT BTC.

Figure 19 shows the observed TNT BTC for Soil C and the fitted semianalytical model results for Freundlich equilibrium sorption. Freundlich equilibrium sorption improved the data fit considerably ($RMS = 1.460 \text{ mg l}^{-1}$) over the fit

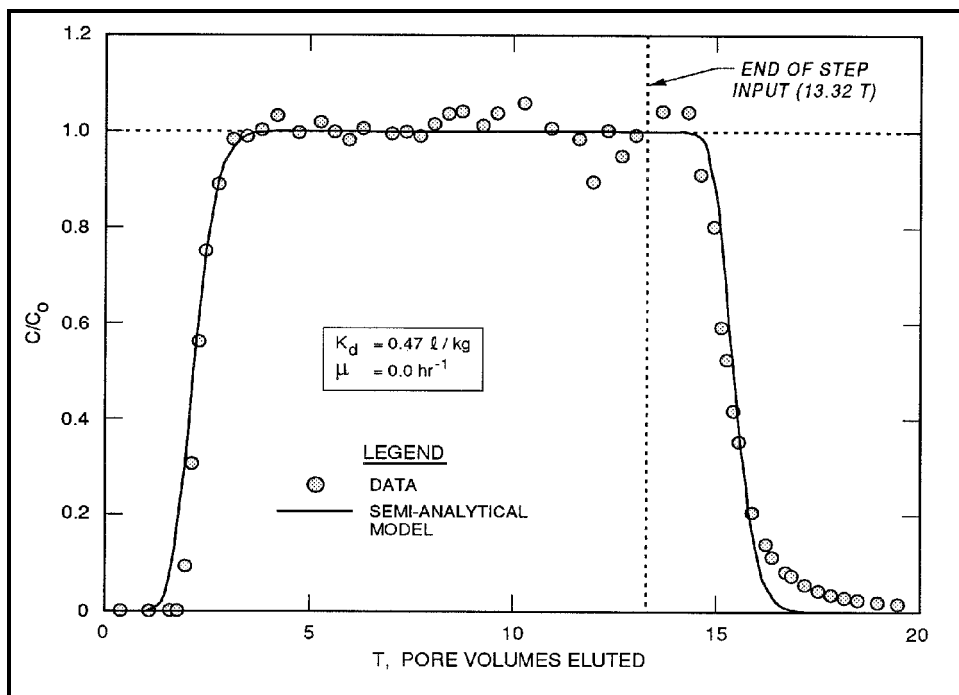


Figure 18. Observed and fitted TNT breakthrough curves for Soil C for linear sorption and first-order transformation

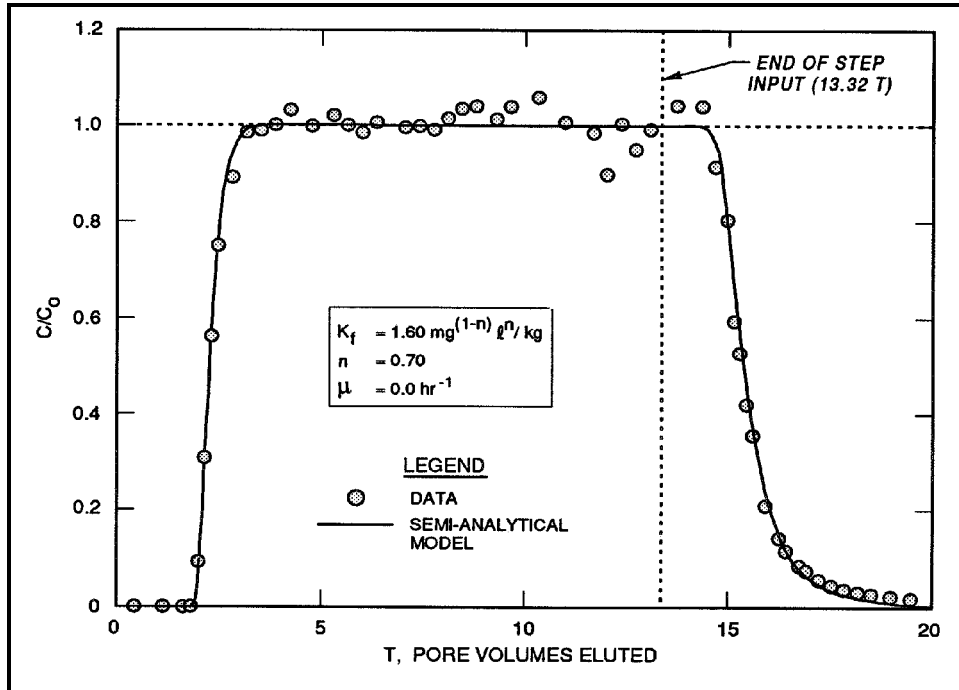


Figure 19. Observed and fitted TNT breakthrough curves for Soil C for Freundlich sorption and first-order transformation

provided by the linear sorption model. Improvement of the fit was due primarily to the ability of the Freundlich model to capture the tailing observed in the BTC. A Freundlich constant (K_f) of $1.6 \text{ mg}^{(1-n)} \ell^n \text{ kg}^{-1}$ and an empirical coefficient (n) of 0.70 were obtained.

Figure 20 shows the observed TNT BTC for Soil C and the fitted semianalytical model results for Langmuir equilibrium sorption. Langmuir equilibrium sorption did not improve the data fit ($RMS = 1.685 \text{ mg } \ell^{-1}$) over the fit provided by the Freundlich sorption model. The Langmuir sorption model, like the Freundlich model was able to capture most of the tailing shown by the Soil C TNT BTC, although not quite as well as the Freundlich sorption model. A Langmuir constant (K_1) of $0.020 \text{ } \ell/\text{mg}$ and a sorption capacity (Q) of 46.0 mg/kg were obtained.

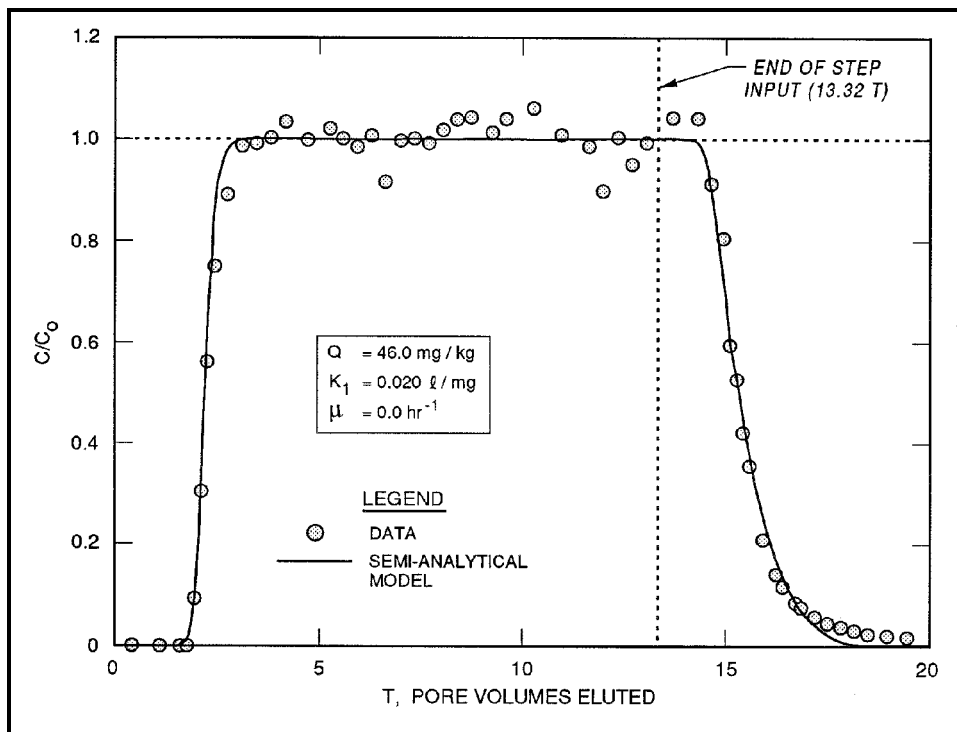


Figure 20. Observed and fitted TNT breakthrough curves for Soil C for Langmuir sorption and first-order transformation

Soil D. Figure 21 shows the observed TNT BTC for Soil D and the fitted semianalytical model results for linear equilibrium sorption and first-order decay. From the steady-state portion of the BTC, a first-order transformation rate constant (μ) of 0.0017 hr^{-1} was obtained. Linear equilibrium sorption, along with first-order transformation, did not provide a very good fit to the Soil D TNT BTC ($RMS = 4.515 \text{ mg } \ell^{-1}$). The model deviated slightly from the observed data near the beginning of the steady-state portion of the BTC. The model also failed to capture the considerable amount of tailing observed in the Soil D BTC. A linear equilibrium distribution coefficient (K_d) of $0.95 \text{ } \ell/\text{kg}$ was obtained for the Soil D TNT BTC.

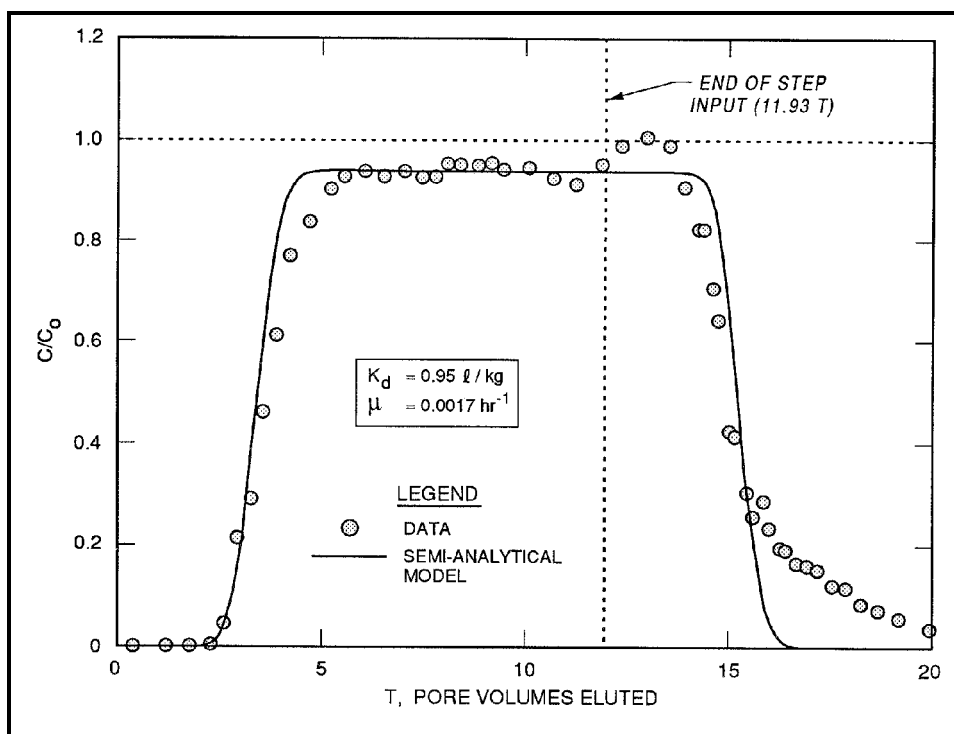


Figure 21. Observed and fitted TNT breakthrough curves for Soil D for linear sorption and first-order transformation

Figure 22 shows the observed TNT BTC for Soil D and the fitted semianalytical model results for Freundlich equilibrium sorption and first-order decay. Freundlich equilibrium sorption improved the fit ($RMS = 3.429 \text{ mg } \ell^{-1}$) over the fit provided by the linear sorption model, due primarily to the ability of the Freundlich model to capture the tailing observed in the BTC. However, the fit to the initial breakthrough portion of the BTC deteriorated with Freundlich sorption as opposed to linear sorption. A Freundlich constant (K_f) of $4.0 \text{ mg}^{(1-n)} \ell^n \text{ kg}^{-1}$ and an empirical coefficient (n) of 0.65 were obtained.

Figure 23 shows the observed TNT BTC for Soil D and the fitted semianalytical model results for Langmuir equilibrium sorption and first-order decay. Langmuir equilibrium sorption did not improve the fit ($RMS = 3.942 \text{ mg } \ell^{-1}$) compared with the fit provided by the Freundlich sorption model. The Langmuir sorption model, like the Freundlich model, was able to capture most of the tailing shown by the Soil D TNT BTC but did not fit the front portion of the BTC well. A Langmuir constant (K_L) of 0.028 l/mg and a sorption capacity (Q) of 80.0 mg/kg were obtained.

Crane soil. Figure 24 shows the observed TNT elution curve for Crane soil and the fitted semianalytical model results for linear equilibrium sorption and first-order decay. Linear equilibrium sorption with first-order decay could not simulate the persistence in TNT concentrations ($RMS = 0.149 \text{ mg } \ell^{-1}$). A linear equilibrium distribution coefficient (K_d) of 6.0 l/kg and a first-order decay rate constant (μ) of 0.029 hr^{-1} were obtained for the Crane soil TNT elution curve.

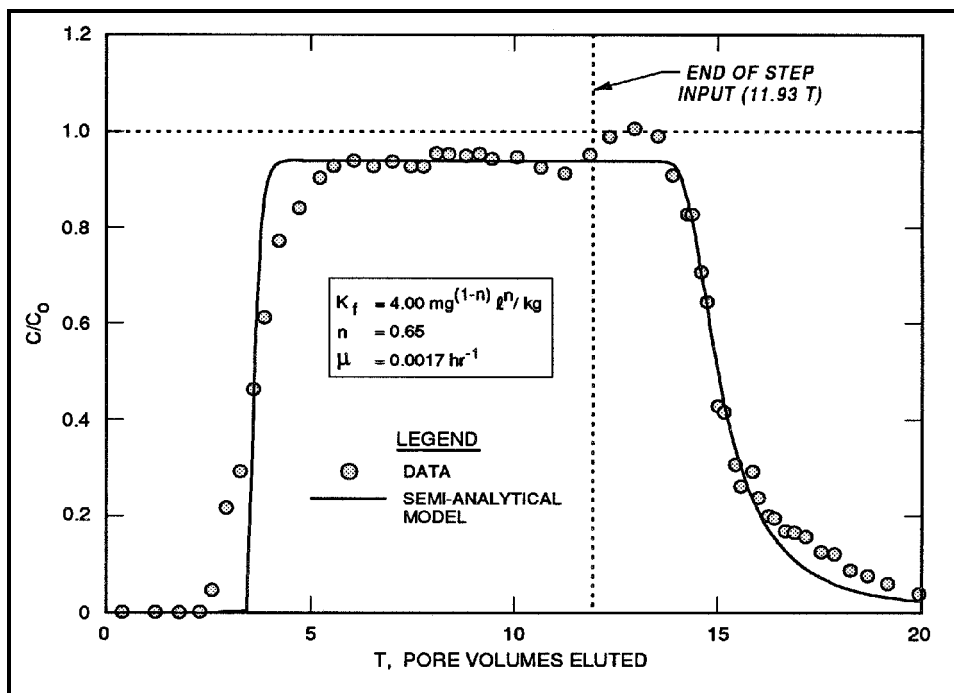


Figure 22. Observed and fitted TNT breakthrough curves for Soil D for Freundlich sorption and first-order transformation

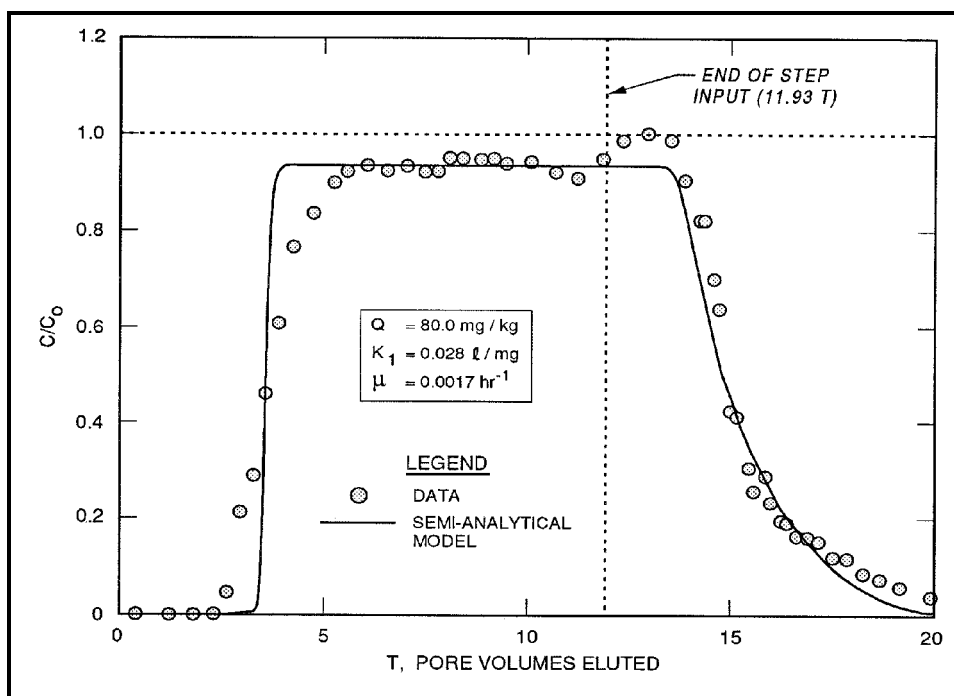


Figure 23. Observed and fitted TNT breakthrough curves for Soil D for Langmuir sorption and first-order transformation

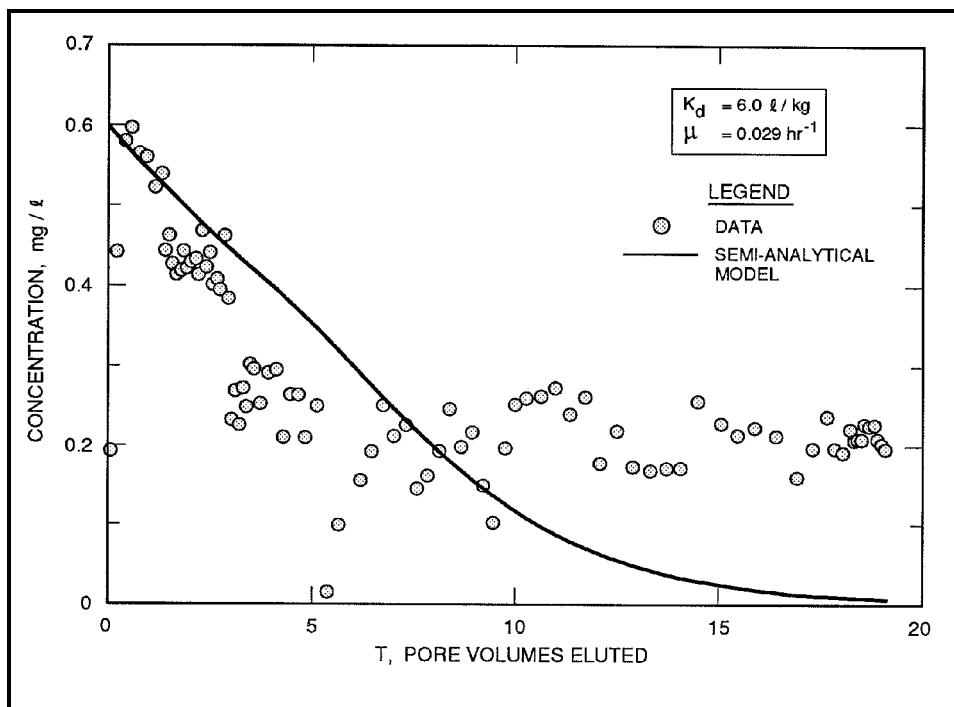


Figure 24. Observed and fitted TNT elution curves for Crane soil for linear sorption and first-order transformation

Figure 25 shows the observed TNT elution curve for Crane soil and the fitted semianalytical model results for Freundlich equilibrium sorption and first-order decay. Freundlich equilibrium sorption improved the fit ($RMS = 0.100 \text{ mg l}^{-1}$) somewhat over the linear sorption model, but still failed to simulate the persistence of TNT concentrations in the leachate. A Freundlich constant (K_f) of $20 \text{ mg}^{(1-n)} \text{ l}^n \text{ kg}^{-1}$ and an empirical coefficient (n) of 0.10 were obtained, along with a first-order decay rate constant (μ) of 0.029 hr^{-1} .

Additional improvement was gained ($RMS = 0.085 \text{ mg l}^{-1}$) in the fit between the observed TNT elution curve for Crane soil and the semianalytical model results when Langmuir sorption was used in the semianalytical model (Figure 26). The Langmuir sorption model also failed to capture much of the persistence of TNT concentrations in the leachate, like the Freundlich and linear models. A Langmuir constant (K_1) of 20 l/mg and a sorption capacity (Q) of 18 mg/kg were obtained, along with a first-order decay rate constant (μ) of 0.029 hr^{-1} .

Figure 27 shows the observed TNT elution curve for Crane soil and the fitted semianalytical model results for film diffusion, linear equilibrium sorption, and first-order decay. Addition of the film diffusion term allowed the model to simulate the persistence in TNT effluent concentrations ($RMS = 0.068 \text{ mg l}^{-1}$). A linear equilibrium distribution coefficient of 1.8 l/kg , a film coefficient of $5.0 \times 10^{-5} \text{ l/kg/hr}$, and a decay rate constant of 0.03 hr^{-1} were obtained from the curve fit.

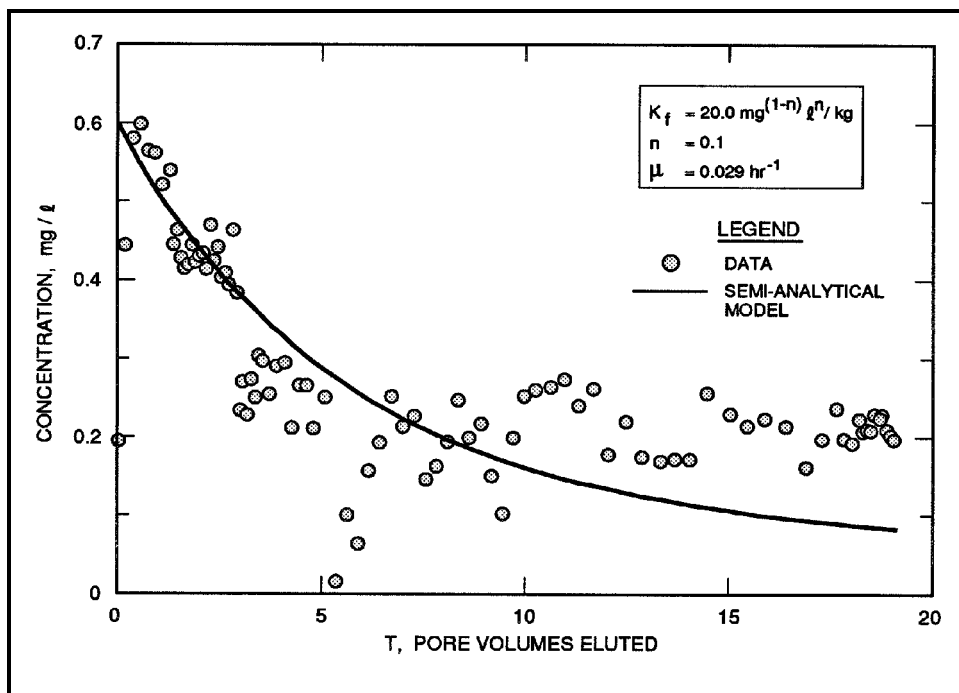


Figure 25. Observed and fitted TNT elution curves for Crane soil for Freundlich sorption and first-order transformation

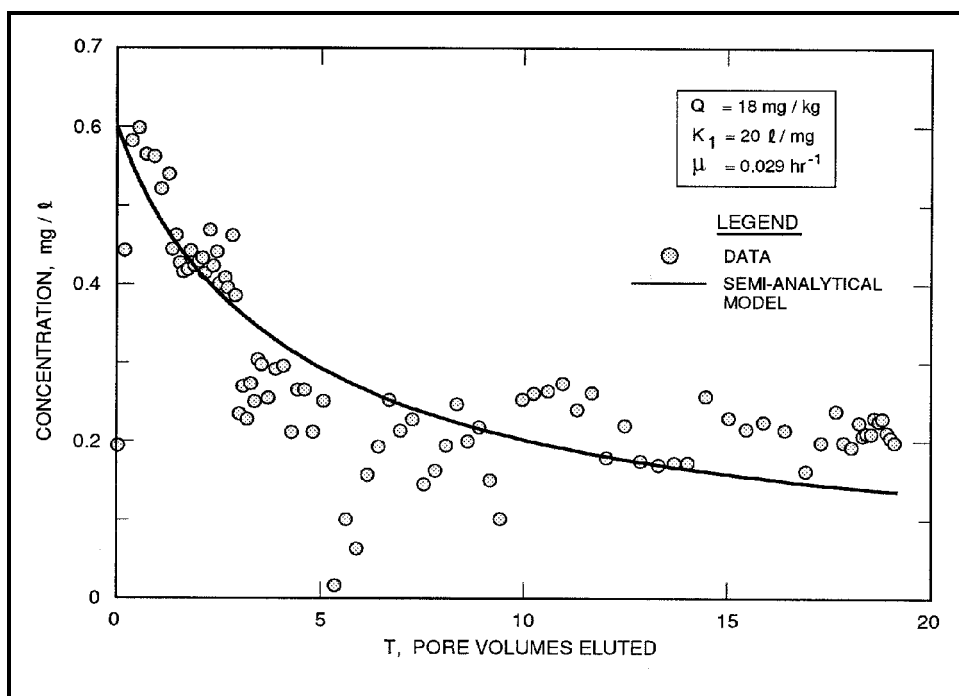


Figure 26. Observed and fitted TNT elution curves for Crane soil for Langmuir sorption and first-order transformation

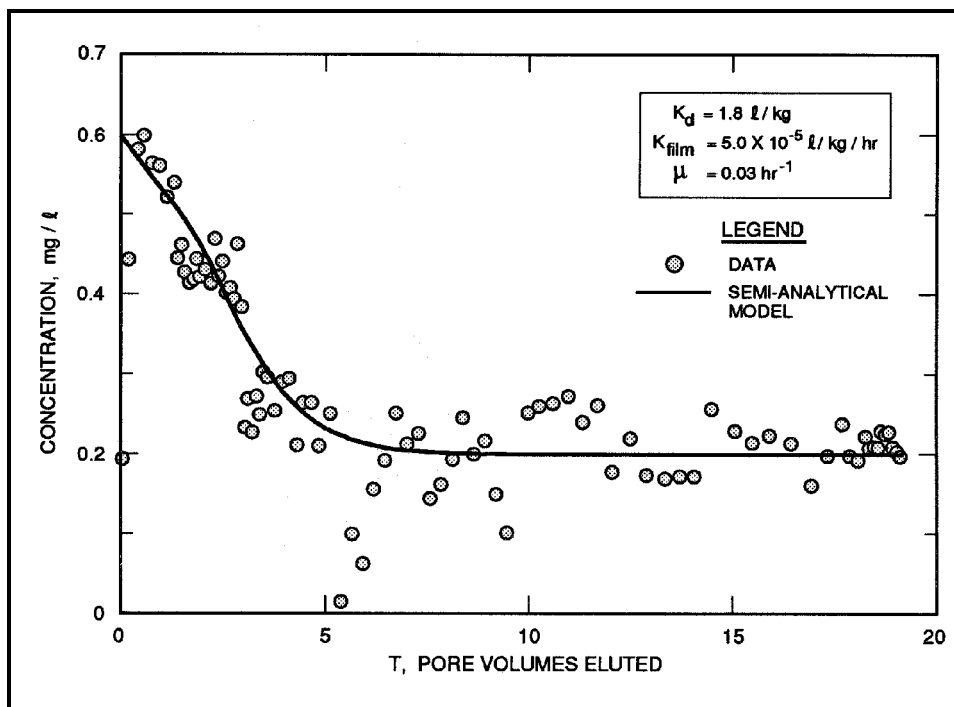


Figure 27. Observed and fitted TNT elution curves for Crane soil for film diffusion, linear sorption, and first-order transformation

Summary. The TNT BTCs for Soils A, B, and C were fitted adequately using the semianalytical model with first-order decay and nonlinear equilibrium sorption. Both the Freundlich and Langmuir sorption models improved the fits as compared with the linear model. The Langmuir model fit the TNT BTCs from Soils A and B slightly better than the Freundlich model. The opposite was true for the TNT BTCs from Soils C and D. Although nonlinear sorption improved the overall fit to the Soil D BTC compared with linear sorption, the goodness of fit to the initial breakthrough portion of the Soil D BTC was diminished by the addition of nonlinear sorption. TNT sorption and transformation parameters and *RMS* values estimated from the BTCs are summarized in Table 4.

Good TNT mass balances (Table 5) for Soils A, B, C, and D suggest that the estimates of sorption and transformation parameters are credible. Between 96.1 and 105.9 percent of TNT introduced to the soils were accounted for as TNT and TNT transformation products.

The Crane elution curve could not be simulated well using first-order decay with linear, Freundlich, or Langmuir equilibrium sorption models. This was primarily due to the persistence in TNT concentrations in eluate from the Crane soil. Addition of a descriptor for dissolution (film diffusion model), along with linear equilibrium sorption and first-order decay, however, enabled the semianalytical model to capture this persistence. TNT sorption and transformation parameters and *RMS* values estimated from the Crane leaching curve are summarized in Table 4.

Table 4
TNT Sorption and Transformation Parameters and *RMS* Values¹
Estimated from the BTCs for Soils A, B, C, and D and from the
Elution Curve for Crane Soil

Soil	A	B	C	D	Crane
Linear Sorption					
μ (hr ⁻¹)	0.0011	0.0000	0.0000	0.0017	0.029
K_d (l/kg)	0.12	0.11	0.47	0.95	6.0
<i>RMS</i> (mg l ⁻¹)	1.856	2.973	3.214	4.515	0.149
Freundlich Sorption					
μ (hr ⁻¹)	0.0011	0.0000	0.0000	0.0017	0.029
K_f (mg ⁽¹⁻ⁿ⁾ l ⁿ kg ⁻¹)	0.45	0.38	1.6	4.0	20
<i>n</i>	0.73	0.73	0.70	0.65	0.10
<i>RMS</i> (mg l ⁻¹)	1.775	2.199	1.460	3.429	0.100
Langmuir Sorption					
μ (hr ⁻¹)	0.0011	0.0000	0.0000	0.0017	0.029
K_1 (l/mg)	0.04	0.045	0.020	0.028	20
<i>Q</i> (mg/kg)	9.0	9.0	46.0	80	18
<i>RMS</i> (mg l ⁻¹)	1.265	1.857	1.685	3.942	0.085
Film Model					
μ (hr ⁻¹)	---	---	---	---	0.03
K_d (l/kg)	---	---	---	---	1.8
K_{film} (hr ⁻¹)	---	---	---	---	5.0×10^{-5}
<i>RMS</i> (mg l ⁻¹)	---	---	---	---	0.068

¹ Shading indicates the best *RMS* value for each soil.

Table 5
TNT Mass Balance¹

Soil	A	B	C	D
TNT as TNT eluted	97.6	105.1	100.7	95.1
TNT residual ²	0.0	0.0	0.1	0.0
TNT as 2A-DNT eluted	0.3	0.3	0.2	0.2
TNT as 4A-DNT eluted	0.7	0.5	0.3	0.8
Total	98.6	105.9	101.3	96.1

¹ Computed on a molar basis and normalized for a total molar input of 100.

² TNT remaining in soil after completion of experiment.

Discussion

The Moldrup et al. (1992) and Yamaguchi et al. (1994) semianalytical model was easily implemented in MathCAD. Various process descriptors were incorporated into the model with minimal modifications. Investigation of the applicability of nonlinear descriptors to laboratory soil column data was possible with the semianalytical model. The ability to incorporate nonlinear process descriptors makes the semianalytical model much more flexible than fully analytical solutions, which are restricted to linear descriptors. Extensive knowledge of computer programming, which is often needed with fully numerical solutions, was not required in implementing the semianalytical model. Comparisons of the semianalytical model to two analytical solutions and one numerical model indicated that the semianalytical model was properly implemented in MathCAD.

Equilibrium sorption and first-order transformation were adequate process descriptors for simulating the TNT BTCs for Soils A, B, and C. Nonlinear sorption descriptors (Freundlich and Langmuir) improved the overall fit for each BTC over fits provided by a linear sorption descriptor. Improvement of the fits was due primarily to the ability of the nonlinear descriptors to capture tailing near the end of washout. The Freundlich sorption descriptor fit the BTCs for Soils A and B slightly better than the Langmuir sorption descriptor. Conversely, the Langmuir descriptor fit the BTCs for Soils C and D slightly better than the Freundlich descriptor. Differences between the Freundlich and Langmuir fits did not appear significant. A nonlinear descriptor for TNT sorption is consistent with much of the column data and most batch isotherms reported in the literature (Townsend and Myers 1996). Batch isotherms in the literature are also divided between Freundlich and Langmuir descriptors, as were the model fits for the soils here.

Freundlich and Langmuir sorption descriptors improved the overall fits for Soils A, B, C, and D by allowing the model to capture the tailing near the end of washout. The fit to the initial breakthrough portion of the Soil D BTC, however, was worsened by the nonlinear descriptors compared with the fit obtained for linear sorption. Since Freundlich or Langmuir sorption could not improve the washout portion of the Soil D BTC without decreasing the goodness of fit to the initial breakthrough portion of the BTC, a descriptor other than Freundlich or Langmuir equilibrium sorption may be needed to fully describe TNT transport in the Soil D column.

BTC asymmetry may be caused by physical phenomena such as mass transfer limitations or chemical reaction phenomena (Brusseau and Rao 1989). Physical nonequilibrium occurs when regions of immobile water exist, and solutes are transported through these regions only by diffusion. Immobile water regions have been conceptualized as intra-aggregate microporosity, dead-end pores, surface films, and matrix porosity of fractured media (Brusseau and Rao 1989).

The Crane soil elution curve showed significant persistence in TNT concentrations that the semianalytical model with equilibrium sorption (linear or nonlinear) and first-order decay could not simulate. This persistence was attributed

to dissolution of crystalline TNT (Pennington et al. 1995), based on the shape of the elution curve and high measured TNT concentrations in one section of soil after elution was completed. Thus, a descriptor for the process of dissolution was added to the semianalytical model. The added dissolution descriptor accounts for mass transfer limitations between two regions of potentially contrasting concentration. For the case of nonequilibrium sorption, the film model accounts for diffusion through films surrounding soil solids. For dissolution, the film model accounts for diffusion through films surrounding contaminant crystals.

The semianalytical model allowed the dissolution process to be investigated for applicability to Crane soil. Addition of a film diffusion descriptor greatly improved the fit compared with the fits obtained when only sorption and transformation processes were accounted for. Thus, the dissolution process appears to be significant for the Crane soil, and the film diffusion model appears to be an accurate descriptor for the dissolution process. It is also possible that the film diffusion model was actually describing nonequilibrium sorption or accounting for some other process, but the data suggest that the dissolution process was applicable to Crane soil.

The good fits obtained from the semianalytical model do not necessarily mean that the process descriptors used are correct. Other processes and/or process descriptors could be involved in the TNT transport process and may provide similar fits to these data. Similarly, processes other than the ones emphasized here may apply for different environmental conditions. Thus, caution should be used when identifying significant processes and developing descriptors for those processes.

4 Conclusions

The Moldrup et al. (1992) and Yamaguchi et al. (1994) semianalytical model is a useful tool for evaluating laboratory soil column data. The model is simple to implement, yet provides the user the ability to apply more complicated process descriptors to soil column data than fully analytical solutions allow. The semi-analytical model allows modification of processes, descriptors, and boundary conditions with minimal effort.

The TNT BTCs for three of four soils were simulated adequately using the semianalytical model with equilibrium sorption and first-order transformation. Freundlich and Langmuir sorption descriptors provided better fits to the BTCs than the linear sorption model, primarily because of the ability of the nonlinear models to capture the tailing observed in the BTCs. Differences in the fits provided by the Freundlich model to fits provided by the Langmuir model appeared to be insignificant for the experimental conditions encountered here. First-order transformation was adequate for the data here, although this might not prove to be the case for other soils and environmental conditions where transformation is more significant.

The elution curve for Crane soil (Pennington et al. 1995) could not be simulated adequately by the semianalytical solution with equilibrium sorption and first-order transformation alone. In addition to equilibrium sorption and first-order transformation, a descriptor for TNT dissolution that accounted for mass transfer limitations through films of immobile water surrounding TNT crystals was needed to adequately simulate the Crane soil elution curve.

Laboratory soil column studies provide information on TNT transport processes, descriptors for these processes, and estimates for parameters quantifying process descriptors. The Moldrup et al. (1992) and Yamaguchi et al. (1994) semianalytical model is an excellent tool for simulating laboratory soil column data, investigating process descriptors, and obtaining process parameters needed for field-scale modeling.

References

- Ainsworth, C. C., Harvey, S. D., Szecsody, J. E., Simmons, M. A., Cullinan, V. I., Resch, C. T., and Mong, G. H. (1993). "Relationship between the leachability characteristics of unique energetic compounds and soil properties," Final Report, Project Order No. 91PP1800, U.S. Army Biomedical Research and Development Laboratory, Fort Detrick, Frederick, MD.
- Bear, J. (1972). *Dynamics of fluids in porous media*. American Elsevier Publishing Company, New York.
- Brusseau, M. L., and Rao, P. S. C. (1989). "Sorption nonideality during organic contaminant transport in porous media," *CRC Critical Reviews in Environmental Control* 19, 33-99.
- Cleary, R. W., and Adrian, D. D. (1973). "Analytical solution of the convective-dispersive equation for cation adsorption in soils," *Soil Science Society of America Proceedings* 19, 197-199.
- Comfort, S. D., Shea, P. J., Hundal, L. S., Li, Z., Woodbury, B. L., Martin, J. L., and Powers, W. L. (1995). "TNT transport and fate in contaminated soil," *Journal of Environmental Quality* 24, 1174-1182.
- Domenico, P. A., and Schwartz, F. W. (1990). *Physical and chemical hydrogeology*. John Wiley and Sons, New York.
- Grove, D. B., and Stollenwerk, K. G. (1984). "Computer model of one-dimensional equilibrium-controlled sorption processes," Water Resources Investigations Report 84-4059, U.S. Geological Survey, Denver, CO.
- Jenkins, T. F., Miyares, P. H., and Walsh, M. E. (1988). "An improved RP-HPLC method for determining nitroaromatics and nitroamines in water," CRREL Report 88-23, U.S. Army Cold Regions Research and Engineering Laboratory, Hanover, NH.
- Jenkins, T. F., and Walsh, M. E. (1987). "Development of an analytical method for explosive residues in soil," CRREL Report 87-7, U.S. Army Cold Regions Research and Engineering Laboratory, Hanover, NH.

- McGrath, C. J. (1995). "Review of formulations for processes affecting the subsurface transport of explosives," Technical Report IRRP-95-2, U.S. Army Engineer Waterways Experiment Station, Vicksburg, MS.
- Moldrup, P., Yamaguchi, T., Hansen, J. A., and Rolston, D. E. (1992). "An accurate and numerically stable model for one-dimensional solute transport in soils," *Soil Science* 153, 261-273.
- Myers, T. E., Brannon, J. M., Pennington, J. C., Townsend, D. M., Davis, W. M., Ochman, M. K., Hayes, C. A., and Myers, K. F. "Laboratory studies of soil sorption/transformation of TNT, RDX, and HMX," Technical Report in preparation, U.S. Army Engineer Waterways Experiment Station, Vicksburg, MS.
- Olin, T. J., Myers, T. E., and Townsend, D. M. (1996). "2,4,6-Trinitrotoluene (TNT) transformation/sorption in thin-disk soil columns under anaerobic conditions," Technical Report IRRP-96-6, U.S. Army Engineer Waterways Experiment Station, Vicksburg, MS.
- Pennington, J. C., Myers, T. E., Davis, W. M., Olin, T. J., McDonald, T. A., Hayes, C. A., and Townsend, D. M. (1995). "Impacts of sorption on in situ bioremediation of explosives-contaminated soils," Technical Report IRRP-95-1, U.S. Army Engineer Waterways Experiment Station, Vicksburg, MS.
- Pugh, D. L. (1982). "Milan Army Ammunition Plant contamination survey," Aberdeen Proving Ground: U.S. Army Toxic and Hazardous Materials Agency, USATHAMA Report DRXTH-FR-8213.
- Ro, K. S., Venugopal, A., Adrian, D. D., Constant, D., Qaisi, K., Valsaraj, K. T., Thibodeaux, L. J., and Roy, D. (1996). "Solubility of 2,4,6-trinitrotoluene (TNT) in water," *Journal of Chemical and Engineering Data* 41(4), 758-761.
- Selim, H. M., Amacher, M. C., and Iskandar, I. K. (1990). "Modeling the transport of heavy metals in soils," CRREL Monograph 2, U.S. Government Printing Office.
- Selim, H. M., Xue, S. K., and Iskandar, I. K. (1995). "Transport of 2,4,6-trinitrotoluene and hexahydro-1,3,5-trinitro-1,3,5-triazine in soils," *Soil Science* 160(5), 328-339.
- Spalding, R. F., and Fulton, J. W. (1988). "Groundwater munition residues and nitrate near Grand Island, Nebraska, U.S.A.," *Journal of Contaminant Hydrology* 2, 139-153.
- Townsend, D. M., and Myers, T. E. (1996). "Recent developments in formulating model descriptors for subsurface transformation and sorption of TNT, RDX, and HMX," Technical Report IRRP-96-1, U.S. Army Engineer Waterways Experiment Station, Vicksburg, MS.

- Townsend, D. M., Myers, T. E., and Adrian, D. D. (1995). "2,4,6-Trinitrotoluene (TNT) transformation/sorption in thin-disk soil columns," Technical Report IRRP-95-4, U.S. Army Engineer Waterways Experiment Station, Vicksburg, MS.
- U.S. Army Corps of Engineers. (1970). "Laboratory soils testing," Engineer Manual 1110-2-1906, Washington, DC.
- van Genuchten, M. Th. (1981). "Non-equilibrium transport parameters from miscible displacement experiments," Report 119, U.S. Salinity Laboratory, U.S. Department of Agriculture, Riverside, CA.
- van Genuchten, M. Th., and Alves, W. J. (1982). "Analytical solutions of the one-dimensional convective-dispersive solute transport equation," Technical Bulletin No. 1661, U.S. Salinity Laboratory, U.S. Department of Agriculture, Riverside, CA.
- Yamaguchi, T., Moldrup, P., Rolston, D. E., and Petersen, L. W. (1994). "A semi-analytical solution for one-dimensional solute transport in soils," *Soil Science* 158, 14-21.

Appendix A

Example of MathCad

Implementations for

Semianalytical Model

Soil A

(Freundlich sorption and first-order transformation)

Observed Data		Input soil properties	
$C_{obs} :=$	0.0	0.394	$\rho_b := 1.152$ \leftarrow bulk density, kg/l
	0.0	0.619	
	0.0	0.783	$\theta := 0.53$ \leftarrow porosity
	6.55	1.085	$D := 4.4 \cdot 10^{-5}$ \leftarrow dispersion coefficient, cm ² /sec
	15.0	1.189	
	23.9	1.294	
	29.7	1.403	
	37.4	1.517	
	39.6	1.63	
	43.1	1.961	
	44.0	2.198	
	44.6	2.434	
	43.8	2.789	
	43.7	3.145	
	44.3	3.501	
	44.0	3.849	
	44.2	4.331	
	45.0	4.565	
	43.9	4.798	
	43.3	5.034	
	44.6	5.383	
	44.7	5.728	
	45.1	5.92	
	44.0	6.208	
	45.0	6.427	
	44.0	6.769	
	44.2	7.128	
	44.4	7.482	
	47.2	7.953	
	46.7	8.416	
	46.8	8.871	
	47.0	9.327	
	46.0	9.676	
	44.4	9.864	
		Column operating parameters	
		$u := 1.3 \cdot 10^{-4}$	\leftarrow pore water velocity, cm/sec
		$L := 15.2$	\leftarrow column length, cm
		$step\ T := 9.74$	\leftarrow pore volumes eluted at end of step input
		$c1 := 45.9$	\leftarrow input concentration before end of step input
		$c2 := 0$	\leftarrow input concentration after end of step input
		$C_0 := 0$	\leftarrow initial solute concentration in the soil

44.4	9.864
45.9	10.233
43.8	10.368
41.8	10.506
35.4	10.644
21.6	10.905
11.6	11.161
6.13	11.425
3.52	11.692
2.36	11.959
1.84	12.095
1.37	12.367
1.14	12.504
0.944	12.774
0.8	12.907
0.685	13.176
0.574	13.445
0.482	13.709
0.417	13.98
0.334	14.247
0.285	14.784
0.258	15.458
0.168	17.189
0.118	19.359

The following function rounds numbers to the nearest integer.

$\text{round}(x) := \text{if}(x - \text{floor}(x) < 0.5, \text{floor}(x), \text{ceil}(x))$

$\text{delta } T := 0.0075$ \leftarrow pore volume increment

$N := \text{rows}(T_{\text{obs}})$ \leftarrow number of data points

$N = 57$

$kk := 0..N - 1$ \leftarrow counter

$T_{\text{obs}_{kk}} := \text{round}\left(\frac{T_{\text{obs}_{kk}}}{\text{delta } T}\right) \cdot \text{delta } T$ \leftarrow rounds pore volume data to the nearest pore volume increment

Input reaction term

$\mu_1 := 3.06 \cdot 10^{-7}$ \leftarrow reaction coefficient, sec^{-1}

$S(c) := \mu_1 \cdot c$ \leftarrow reaction term $\text{mg} \cdot \text{liter}^{-1} \cdot \text{sec}^{-1}$

Input sorption term

$n = .73$ <-- empirical constant
 $K_f = .45$ <-- Freundlich constant, $\text{mg}^{(1-n)} \cdot \text{liter}^n \cdot \text{kg}^{-1}$

$$R_m(c) := \begin{cases} 1 + \left(n \cdot K_f c^{n-1} \right) \cdot \frac{\rho_b}{\theta} & \text{if } c > 0 \\ 1 & \text{otherwise} \end{cases} \quad \text{<-- retardation attributed to sorption, dimensionless}$$

Model Equations

$\beta := \frac{D}{u}$ <-- solute dispersivity, cm

$\beta = 0.338$

$\Delta z := 0.5$ <-- distance increment, cm

$\Phi_1 := \Delta T \cdot L$ <-- solute unit mean travel distance

$\Phi_1 = 0.114$

$\max T := 25$ <-- maximum number of pore volumes

$\Delta t := \Delta T \cdot \frac{L}{u}$ <-- time increment

$\Delta t = 876.923$

Stability Criteria

Criterion 1: Φ_1 must be less than $\max \Phi$

$$\max \Phi := \Delta z \cdot \frac{e^{\left(\frac{\Delta z}{\beta} \right)} - 1}{e^{\left(\frac{\Delta z}{\beta} \right)} + 1}$$

$\max \Phi = 0.314$ $\Phi_1 = 0.114$

Criterion 2: Φ_1 must be less than 0.15

$$\Phi_1 = 0.114$$

Criterion 3: Criterion₃ must be between -2 and 2.

$$\text{Criterion}_3 := \frac{1}{\beta} \cdot \left(0.25 + \frac{.5}{\frac{\text{delta}_z}{e^{\frac{\beta}{\beta}} - 1}} \right) - \frac{1}{\beta} \cdot (0.5 \cdot \Phi_1 + \beta)$$

$$\text{Criterion}_3 = 7.163 \cdot 10^{-3}$$

$$T_{\text{step}} := \text{ceil} \left(\frac{\max T}{\text{delta } T} \right) \quad \leftarrow \text{number of pore volume steps (the ceil function returns the next integer above its argument)}$$

$$T_{\text{step}} = 3.334 \cdot 10^3$$

$$i := 0 .. T_{\text{step}} \quad \leftarrow \text{counter}$$

$$z_{\text{max}} := 50 \quad \leftarrow \text{maximum distance analyzed}$$

$$z_{\text{step}} := \text{ceil} \left(\frac{z_{\text{max}}}{\text{delta } z} \right) \quad \leftarrow \text{maximum number of distance steps}$$

$$z_{\text{step}} = 100$$

$$j := 1 .. z_{\text{step}} - 1 \quad \leftarrow \text{counter}$$

$$d_{\text{step}} := \text{round} \left(\frac{L}{\text{delta } z} \right) \quad \leftarrow \text{distance step at the distance of interest (the round function returns the closest integer to its argument)}$$

$$d_{\text{step}} = 30$$

The following function sets the input concentration equal to c1 for pore volumes less than the step input and equal to c2 for pore volumes greater than the step input.

$$\text{input}(i) := \begin{cases} c1 & \text{if } i \cdot \text{delta } T \leq \text{step } T \\ c2 & \text{if } i \cdot \text{delta } T > \text{step } T \end{cases}$$

$$c_{\text{old},j+1} := C_0$$

$$A(c) := \frac{1}{R_m(c)} \cdot \left(\frac{\Phi_1}{2 \cdot \Delta z} + \frac{\Phi_1^2}{2 \cdot \Delta z^2} + \frac{\beta \cdot \Phi_1}{\Delta z^2} \right)$$

$$B(c) := \frac{1}{R_m(c)} \cdot \left(R_m(c) - \frac{\Phi_1^2}{\Delta z^2} - \frac{2 \cdot \beta \cdot \Phi_1}{\Delta z^2} \right)$$

$$C(c) := \frac{1}{R_m(c)} \cdot \left(-\frac{\Phi_1}{2 \cdot \Delta z} + \frac{\Phi_1^2}{2 \cdot \Delta z^2} + \frac{\beta \cdot \Phi_1}{\Delta z^2} \right)$$

The following function increases the concentration profile (c_{old}) by one pore volume step.

$$f(c_{old}, z_{step}) := \begin{cases} \text{for } j \in 1..z_{step} - 1 \\ m_j \leftarrow A(c_{old_j}) \cdot c_{old_{j-1}} + B(c_{old_j}) \cdot c_{old_j} + C(c_{old_j}) \cdot c_{old_{j+1}} - \frac{S(c_{old_j}) \cdot \Delta t}{R_m(c_{old_j})} \\ \text{for } j \in 1..z_{step} - 1 \\ c_{old_j} \leftarrow m_j \\ c_{old} \end{cases}$$

The following function increases the pore volume steps and saves the concentrations at each pore volume step for the distance of interest.

$$Con(T_{step}, c_{old}) := \begin{cases} \text{for } i \in 1..T_{step} \\ c_{old} \leftarrow f(c_{old}, z_{step}) \\ con_{dep_i} \leftarrow c_{old_{d_{step}}} \\ c_{old_0} \leftarrow input(i) \\ con_{dep} \end{cases}$$

$$Concentration := Con(T_{step}, c_{old})$$

$ii := 0..T_{step}$ \leftarrow counter

$C_{fit_{ii,0}} := ii \cdot \Delta T$ $C_{fit_{ii,1}} := \text{Concentration}_{ii}$

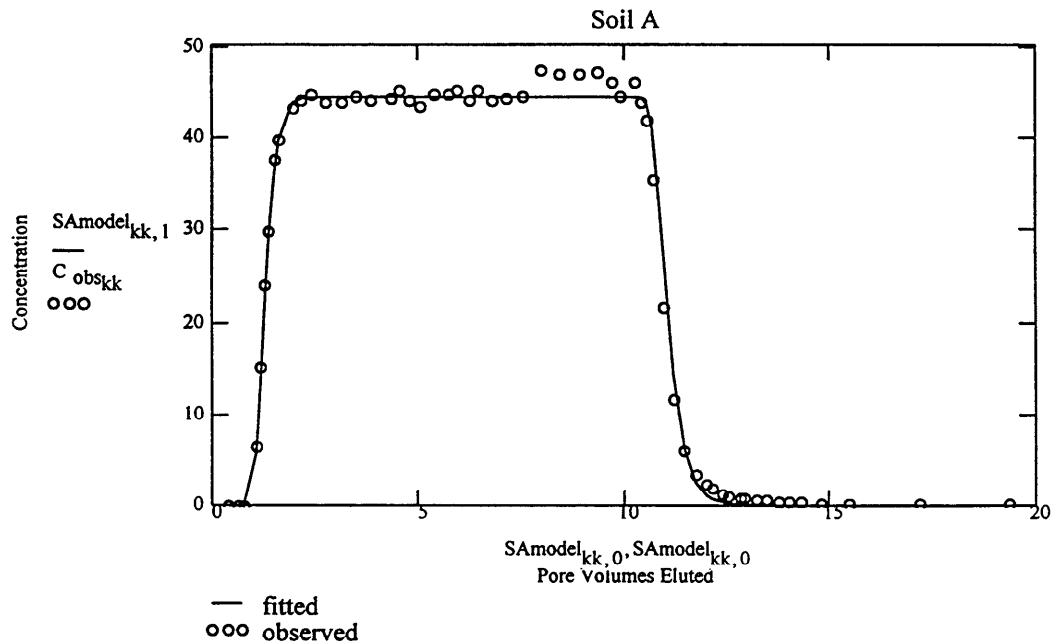
The following function picks out the fitted concentrations that correspond to the observed concentrations.

```

Conc2(N, C_fit, data time) :=
  j ← 0
  for k ∈ 0..N - 1
    while C_fit_{j,0} ≤ T_obs_k
      new_{k,0} ← C_fit_{j,0}
      new_{k,1} ← C_fit_{j,1}
      j ← j + 1
  new

```

$SAmodel := \text{Conc2}(N, C_{fit}, T_{obs})$ \leftarrow semi-analytical model results



REPORT DOCUMENTATION PAGE

Form Approved
OMB No. 0704-0188

Public reporting burden for this collection of information is estimated to average 1 hour per response, including the time for reviewing instructions, searching existing data sources, gathering and maintaining the data needed, and completing and reviewing the collection of information. Send comments regarding this burden estimate or any other aspect of this collection of information, including suggestions for reducing this burden, to Washington Headquarters Services, Directorate for Information Operations and Reports, 1215 Jefferson Davis Highway, Suite 1204, Arlington, VA 22202-4302, and to the Office of Management and Budget, Paperwork Reduction Project (0704-0188), Washington, DC 20503.

1. AGENCY USE ONLY (Leave blank)		2. REPORT DATE July 1998	3. REPORT TYPE AND DATES COVERED Final report	
4. TITLE AND SUBTITLE Application of a Semianalytical Model to TNT Transport in Laboratory Soil Columns			5. FUNDING NUMBERS	
6. AUTHOR(S) Tommy E. Myers, Dan M. Townsend, Benjamin C. Hill				
7. PERFORMING ORGANIZATION NAME(S) AND ADDRESS(ES) U.S. Army Engineer Waterways Experiment Station 3909 Halls Ferry Road, Vicksburg, MS 39180-6199; Louisiana State University Baton Rouge, LA 70803			8. PERFORMING ORGANIZATION REPORT NUMBER Technical Report IRRP-98-7	
9. SPONSORING/MONITORING AGENCY NAME(S) AND ADDRESS(ES) U.S. Army Corps of Engineers Washington, DC 20314-1000			10. SPONSORING/MONITORING AGENCY REPORT NUMBER	
11. SUPPLEMENTARY NOTES Available from National Technical Information Service, 5285 Port Royal Road, Springfield, VA 22161.				
12a. DISTRIBUTION/AVAILABILITY STATEMENT Approved for public release; distribution is unlimited.			12b. DISTRIBUTION CODE	
13. ABSTRACT (Maximum 200 words) <p>Subsurface contamination by 2,4,6-trinitrotoluene (TNT) poses a threat to groundwater resources at many military installations involved in the manufacture and packing of TNT. Technical guidance for modeling the subsurface transport of TNT is needed to support Department of Defense goals for cleanup at these sites. Important aspects of this guidance include identification of significant processes involved, development of descriptors for those processes, and estimation of parameters used to quantify descriptors.</p> <p>This report describes application of the one-dimensional, semianalytical solute transport model to laboratory soil column (LSC) data for the analysis of TNT breakthrough curves (BTCs) and elution curves. The semianalytical model incorporates linear and nonlinear reaction terms into the one-dimensional advection-dispersion equation for solute transport and thereby allows more complicated process descriptors to be evaluated than do the available analytical models. Like the available models, the semianalytical model is readily implemented on desktop computers using commercially available mathematical software and is simpler to use than numerical models.</p> <p style="text-align: right;">(Continued)</p>				
14. SUBJECT TERMS Breakthrough curves Soil sorption Distribution coefficient TNT Mathematical modeling			15. NUMBER OF PAGES 60	
			16. PRICE CODE	
17. SECURITY CLASSIFICATION OF REPORT UNCLASSIFIED	18. SECURITY CLASSIFICATION OF THIS PAGE UNCLASSIFIED	19. SECURITY CLASSIFICATION OF ABSTRACT	20. LIMITATION OF ABSTRACT	

13. (Concluded).

The semianalytical model was applied to TNT BTCs obtained from four soils and to a TNT elution curve for a contaminated soil from a military installation. Process descriptors for sorption and transformation were investigated using the semianalytical model, and parameters for quantifying the process descriptors were estimated by fitting the semianalytical model to the LSC data.

TNT BTCs for three of four soils were simulated adequately with equilibrium sorption and pseudo first-order transformation. Nonlinear descriptors for sorption (Freundlich and Langmuir) provided better fits to the data than a linear sorption descriptor, primarily because of the ability of the nonlinear models to capture tailing observed in the BTCs. Differences between the Freundlich and Langmuir fits were insignificant. The TNT BTC for one soil showed significant asymmetry on both rising and declining limbs that could not be adequately simulated by equilibrium sorption (linear and nonlinear) and pseudo first-order transformation.

The elution curve for the contaminated soil could not be simulated satisfactorily with equilibrium sorption and pseudo first-order transformation alone. A descriptor for TNT dissolution was needed in addition to equilibrium sorption and pseudo first-order transformation to adequately simulate the contaminated soil elution curve.

The one-dimensional, semianalytical model is recommended for application to laboratory soil column data and the development of process descriptors from such data because the model is easy to use and allows for evaluation of complicated process descriptors. Although the model is one-dimensional and therefore has limited applicability to field problems, process descriptors developed from LSC data using the model are anticipated to be useful for structuring two- and three-dimensional numerical models of TNT subsurface transport.